



University of  
**Salford**  
MANCHESTER

# STOKES POLARIMETRY AND MAGNETO OPTICAL PROPERTIES OF NANOSTRUCTURED MATERIALS



University of  
**Salford**  
MANCHESTER

# STOKES POLARIMETRY AND MAGNETO OPTICAL PROPERTIES OF NANOSTRUCTURED MATERIALS

Tiehan Shen 沈铁汉

University of  
**Salford**  
MANCHESTER



# STOKES POLARIMETRY AND MAGNETO OPTICAL PROPERTIES OF NANOSTRUCTURED MATERIALS

Tiehan Shen 沈铁汉

Joule Physics Laboratory

University of  
**Salford**  
MANCHESTER



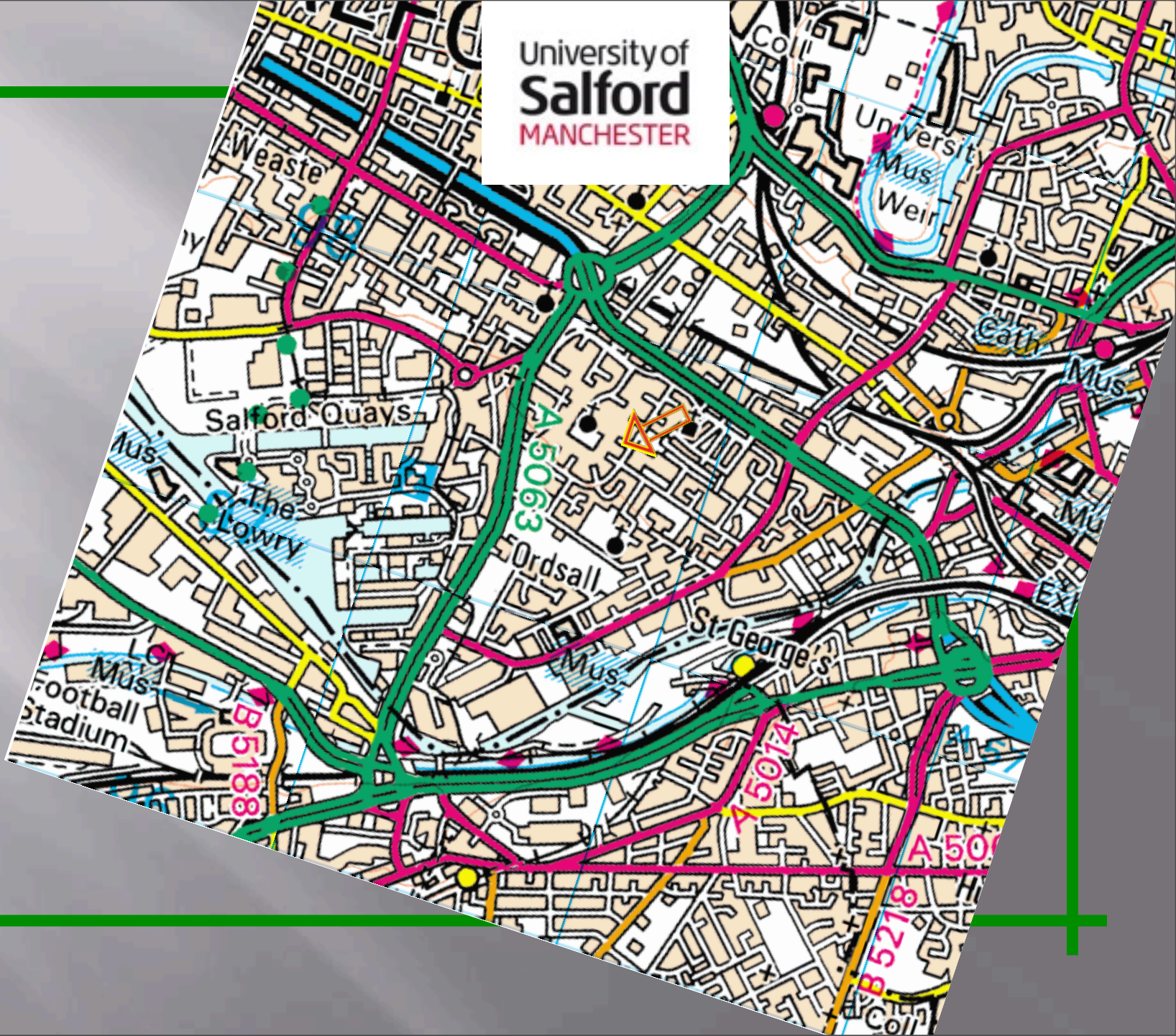
# ABOUT SALFORD...



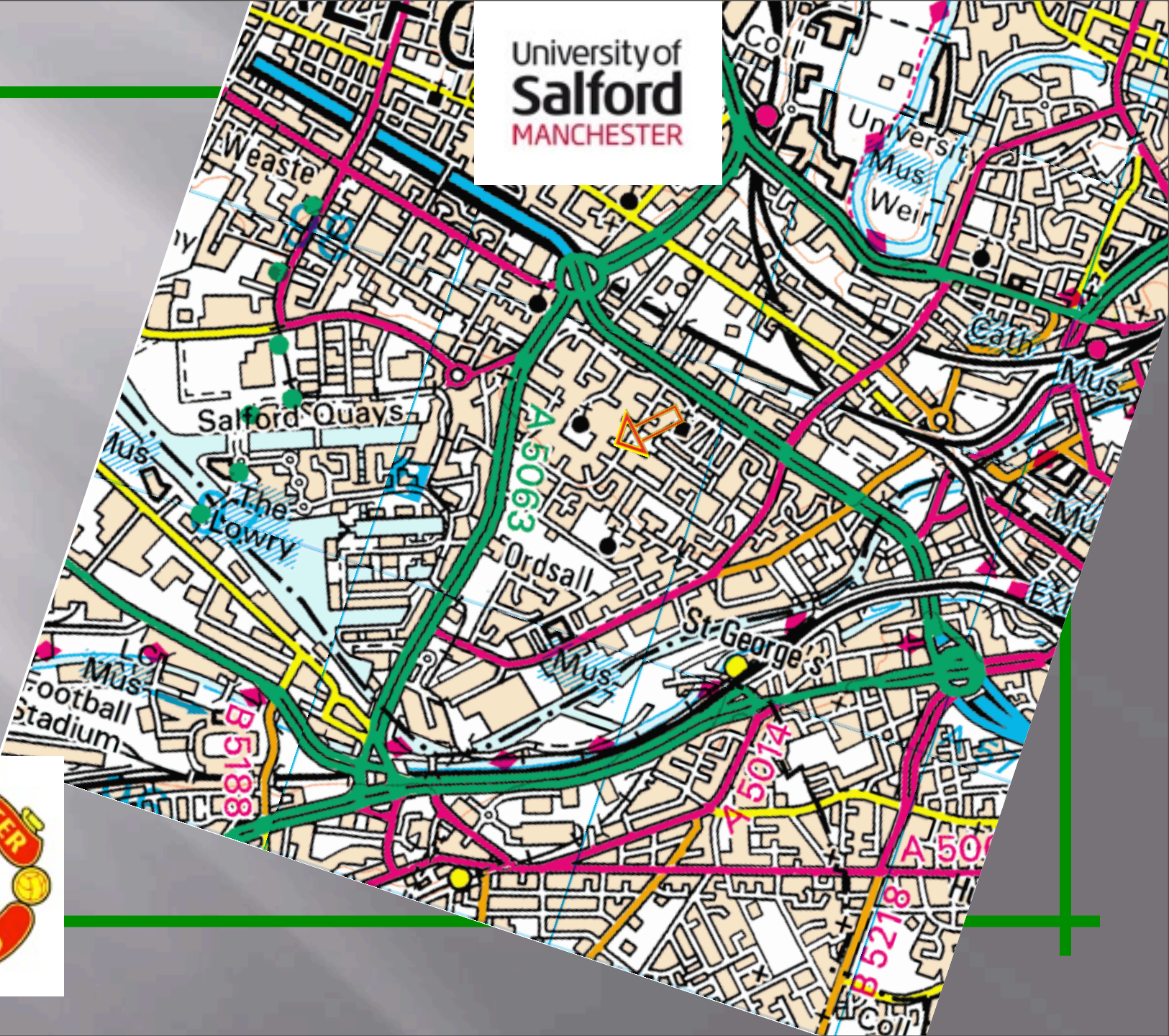




# University of **Salford** MANCHESTER



# University of **Salford** MANCHESTER





L.S. Lowry



Great names associated with Salford include:

L.S. Lowry



Great names associated with Salford include:

L.S. Lowry



Great names associated with Salford include:



L.S. Lowry



Friedrich Engels



Great names associated with Salford include:

L.S. Lowry

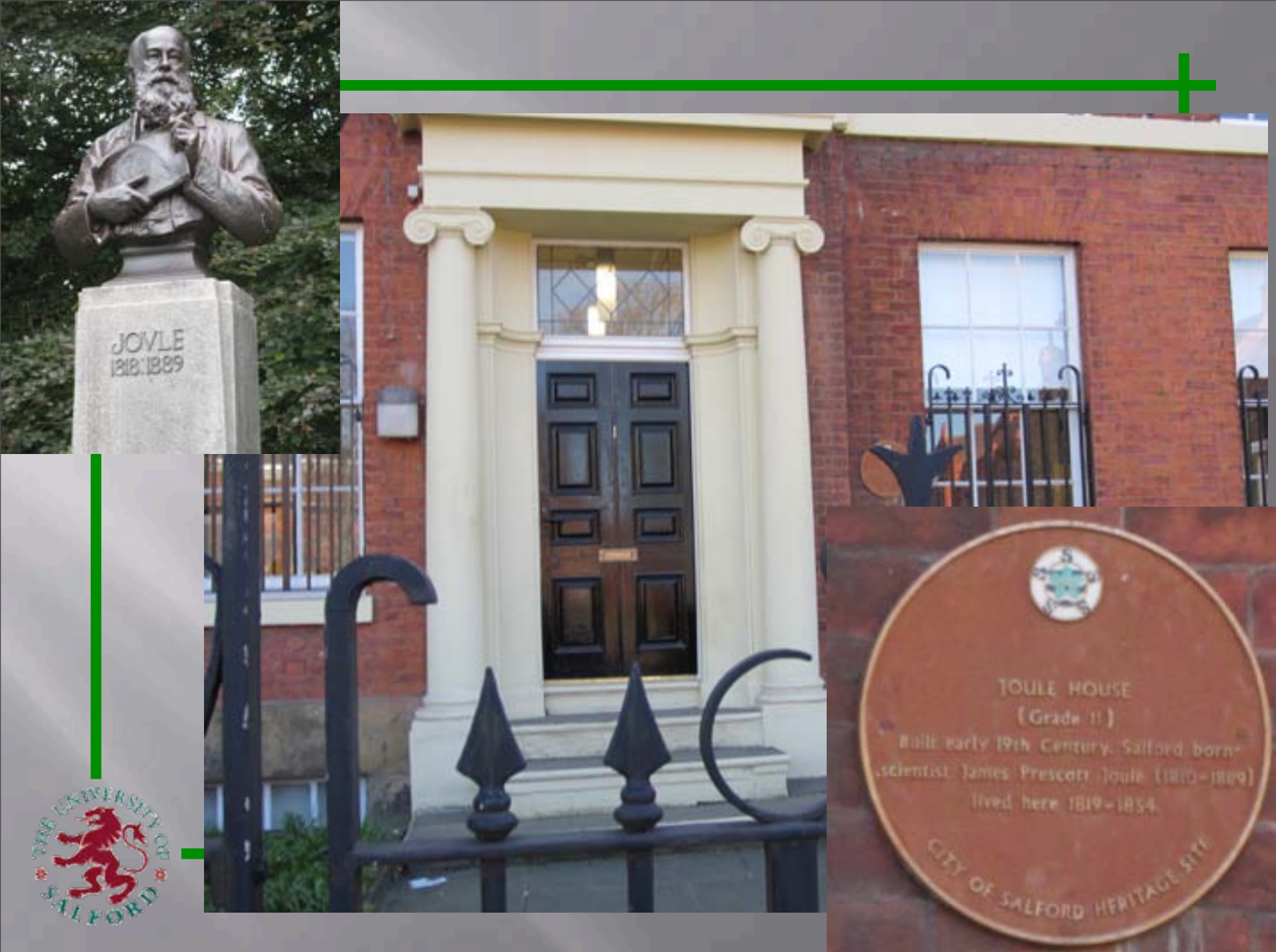


Friedrich Engels



James Prescott Joule

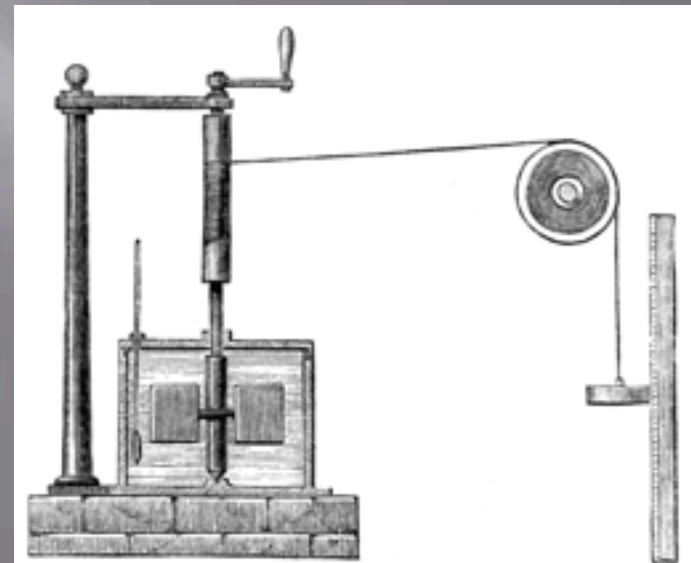




**Joule's contribution to Physics includes:**

**Heating of a current carrying conductor (Joule heating).  
The mechanical equivalent of heat.  
Joule-Thomson effect.**

**The physics laboratory  
is name after the great  
Salfordian physicist.**



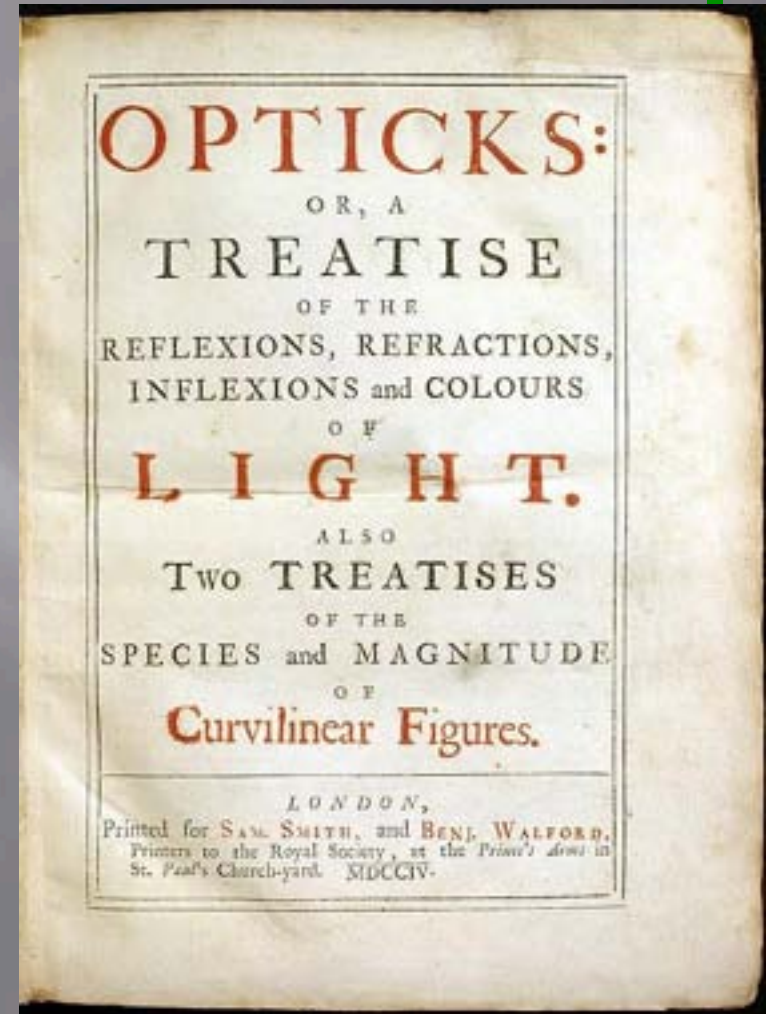
# DETERMINATION OF THE STATE OF POLARISATION OF LIGHT

-the measurement of Stokes  
parameters



# Newton- Opticks: Question 26

- ‘Have not the Rays of Light several sides, endued with several original Properties?’



# the polarisation states of light



- Étienne-Louis Malus was the first to describe the phenomena at the turn of the 19th century when he discovered polarisation by reflection.

# polarisation and the handedness of life?

- Amino acids produced by biological systems are found to be left-handed.
- It has been long speculated that life's preference for left-handed amino acids may have been triggered by compounds brought to Earth by meteorites.
- It has also been speculated that right-handed forms of amino acids in the meteorites could then be preferentially destroyed by circularly polarised light, generated by particles accelerated around neutron stars.



# **Modern exploration of the polarisation characteristics of light has wide-ranging applications**

- biology (e.g. microscopy)
- materials research (e.g. magneto-optical effects)
- environmental monitoring (e.g. aerosol content in atmosphere)
- astronomy (e.g. solar magnetic activity)
- defence (e.g. terrain recognition and landmine detection)



# examples of polarisation analysis in the life sciences

- the study of birefringence signals and calcium transients in skeletal muscles [ Suarez-Kurtz and Parker, Nature 1977]
- imaging of optically active biological structures with circularly polarised light [Keller et al, Proc. Natl, Acad, Sci, USA, 1985], Fibrin architecture in clots [Whittaker and Przyklenk, Blood Cells, Molecules, and Diseases, 2009]
- the imaging of human epithelial properties with polarised light-scattering spectroscopy [Gurjar et al, Nature Medicine 2001]



# Polarisation and Stokes parameters

- The Stokes parameters provide a means whereby the polarisation state of an arbitrary light beam can be uniquely characterised. Techniques used to measure the Stokes parameters are therefore of great interest to those working in the fields of fundamental and applied optics.



## ■ The polarisation ellipse

$$E_x = A_x \cos(kz - \omega t + \delta_x)$$

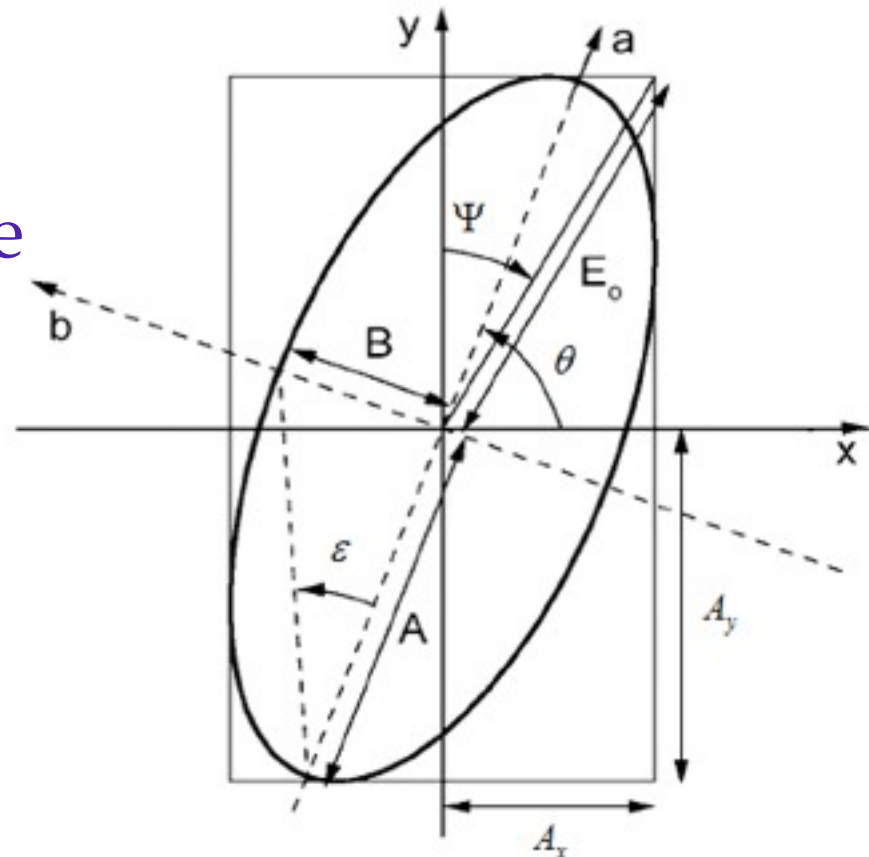
$$E_y = A_y \cos(kz - \omega t + \delta_y)$$

$$A_y^2 E_x^2 + A_x^2 E_y^2 - 2 A_x A_y E_x E_y \cos\delta = A_x^2 A_y^2 \sin^2 \delta$$

$$\tan 2\theta = \tan 2\Psi \cdot \cos\delta$$

$$\sin 2\varepsilon = \sin 2\Psi \cdot \sin\delta$$

$$\tan \Psi \cdot e^{i\delta} = \frac{\tan \theta - i \tan \varepsilon}{1 + i \tan \theta \times \tan \varepsilon}$$



# The Stokes parameters

- A representation was introduced by Stokes in 1852 that the polarisation could be completely represented by four measurable quantities, now known as Stokes parameters.

$$S = \begin{pmatrix} I \\ Q \\ U \\ V \end{pmatrix} = \begin{pmatrix} I_0 \\ I_x - I_y \\ I_{45^\circ} - I_{-45^\circ} \\ I_L - I_R \end{pmatrix} = \begin{pmatrix} A_x^2 + A_y^2 \\ A_x^2 - A_y^2 \\ 2A_x A_y \cos\delta \\ 2A_x A_y \sin\delta \end{pmatrix}$$



**The orientation angle of the polarised light:**

$$\tan 2\theta = \frac{2A_x A_y \cos \delta}{A_x^2 - A_y^2} = \frac{U}{Q}$$

**The ellipticity angle:**

$$\sin 2\varepsilon = \frac{V}{\sqrt{Q^2 + U^2 + V^2}} \text{ or } = \frac{V}{I} (\text{completely-polarised})$$

**Degree of polarisation:**

$$P = \frac{I_{\text{polarised}}}{I_{\text{total}}} = \frac{\sqrt{Q^2 + U^2 + V^2}}{I}$$

**Degree of linear polarisation:**

$$P_{\text{linear}} = \frac{\sqrt{Q^2 + U^2}}{I}$$

**Degree of circular polarisation:**

$$P_{\text{circular}} = \frac{V}{I}$$



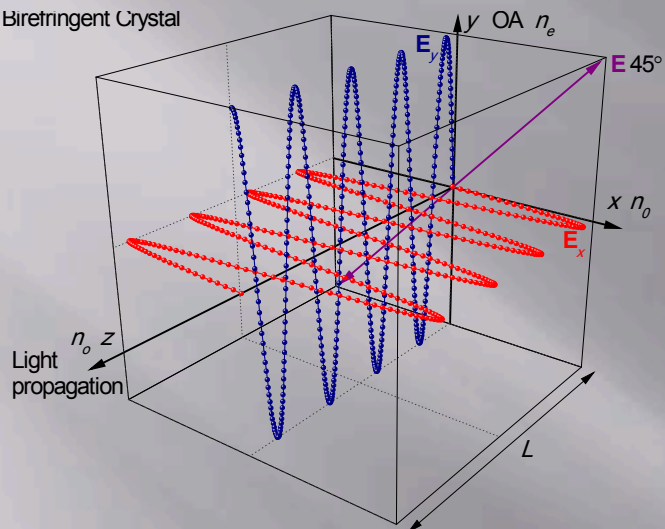
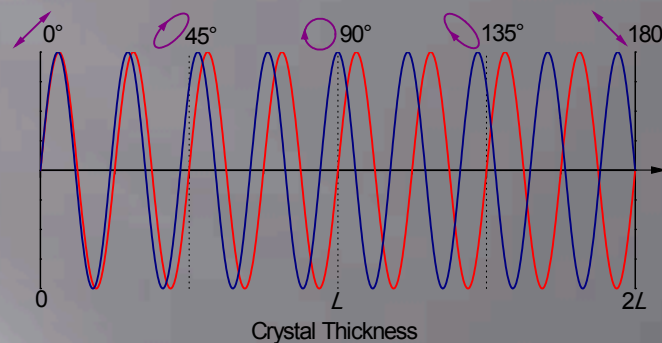
# Phase modulation technique

- An additional linear birefringence is introduced to an optical element.
- This can be achieved by using a liquid crystal electrooptical modulator, a ferroelectric modulator, a Pockel cell or a photoelastic modulator.
- A photoelastic modulator (PEM) is based on the photoelastic effect, in which an optical element will exhibit a degree of birefringence which is proportional to the applied strain.

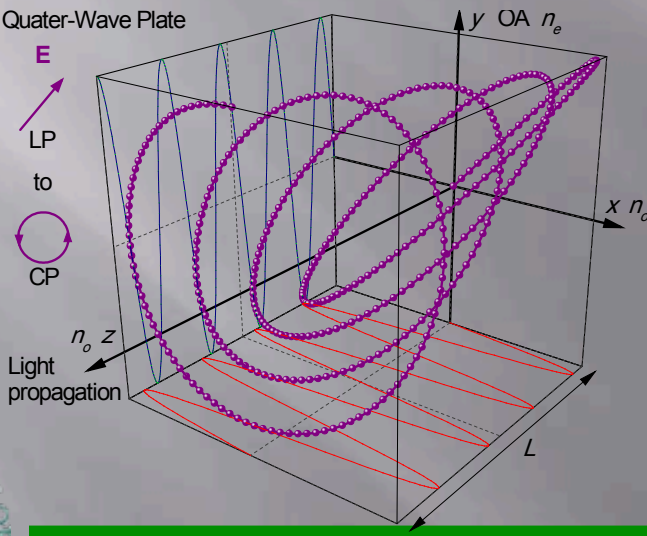


**A**

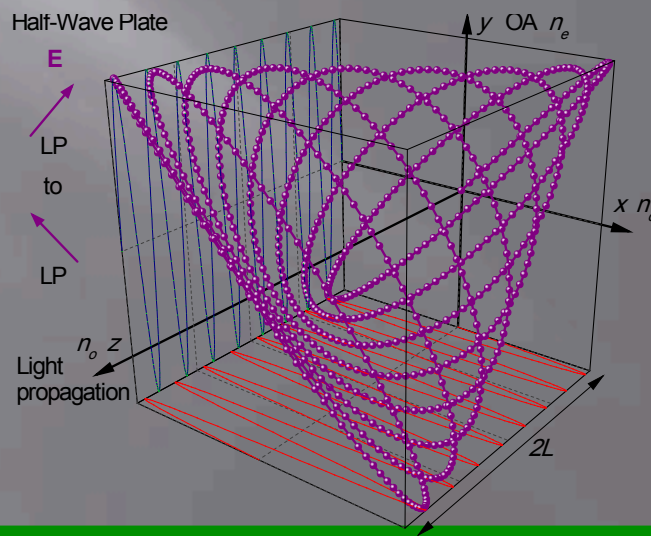
Birefringent Crystal

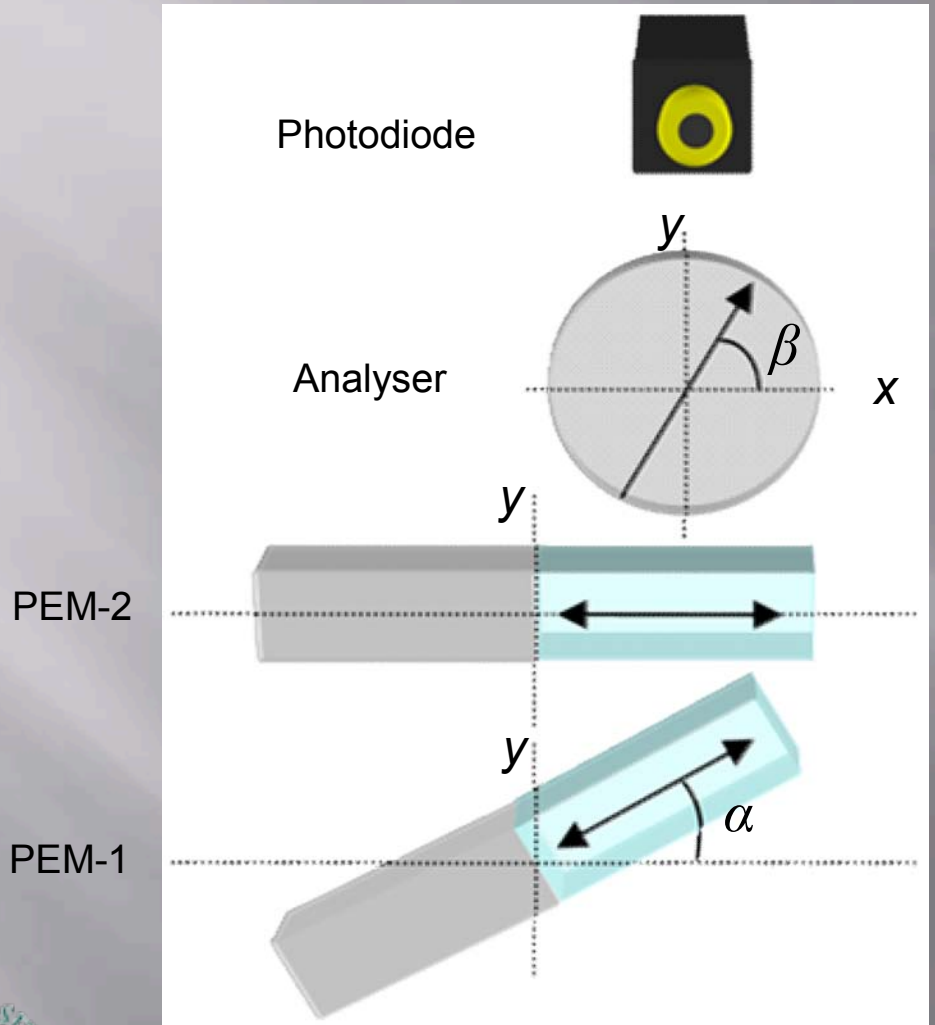
**B**Phase difference between  $E_x$  and  $E_y$  increases with crystal thickness**C**

Quater-Wave Plate

**D**

Half-Wave Plate





A dual photoelastic modulator (PEM) polarimeter showing the 1st PEM, the 2nd PEM, a polarisation analyser and a photodetector.

- A PEM can be treated as a retarder, and when it is rotated by an angle  $\alpha$  from the x-axis, the Mueller matrix for PEM1 can be written as follows,

$$M_1 = \begin{pmatrix} 1 & 0 & 0 & 0 \\ 0 & \cos 4\alpha \cdot \sin^2 \frac{\delta_1}{2} + \cos^2 \frac{\delta_1}{2} & \sin 4\alpha \cdot \sin^2 \frac{\delta_1}{2} & -\sin 2\alpha \cdot \sin \delta_1 \\ 0 & \sin 4\alpha \cdot \sin^2 \frac{\delta_1}{2} & -\cos 4\alpha \cdot \sin^2 \frac{\delta_1}{2} + \cos^2 \frac{\delta_1}{2} & \cos 2\alpha \cdot \sin \delta_1 \\ 0 & \sin 2\alpha \cdot \sin \delta_1 & -\cos 2\alpha \cdot \sin \delta_1 & \cos \delta_1 \end{pmatrix}$$



- For PEM2,  $\alpha=0$ , so the Mueller matrix for this PEM takes the form:

$$M_2 = \begin{pmatrix} 1 & 0 & 0 & 0 \\ 0 & 1 & 0 & 0 \\ 0 & 0 & \cos\delta_2 & \sin\delta_2 \\ 0 & 0 & -\sin\delta_2 & \cos\delta_2 \end{pmatrix}$$



- For the analyser, at angle  $\beta$  with respect to x-axis, the Mueller matrix is:

$$M_3 = \frac{1}{2} \begin{pmatrix} 1 & \cos 2\beta & \sin 2\beta & 0 \\ \cos 2\beta & \cos^2 2\beta & \cos 2\beta \times \sin 2\beta & 0 \\ \sin 2\beta & \cos 2\beta \times \sin 2\beta & \sin^2 2\beta & 0 \\ 0 & 0 & 0 & 0 \end{pmatrix}$$

- and

$$\begin{pmatrix} I' \\ Q' \\ U' \\ V' \end{pmatrix} = M_3 M_2 M_1 \begin{pmatrix} I \\ Q \\ U \\ V \end{pmatrix}$$



$$\begin{aligned}
I' = & \frac{1}{2} I + \frac{1}{2} Q \cos^2 2\alpha \times \cos 2\beta + \frac{1}{4} U \sin 4\alpha \times \cos 2\beta \\
& - \frac{1}{2} V \sin 2\alpha \cdot \cos 2\beta \cdot \sin \delta_1 \\
& + \left( \frac{1}{2} Q \sin^2 2\alpha \cdot \cos 2\beta - \frac{1}{4} U \sin 4\alpha \cdot \cos 2\beta \right) \cdot \cos \delta_1 \\
& + \left( \frac{1}{4} Q \sin 4\alpha \times \sin 2\beta + \frac{1}{2} U \sin^2 2\alpha \times \sin 2\beta \right) \times \cos \delta_2 \\
& + \left( \frac{1}{2} Q \sin 2\alpha \cdot \sin 2\beta - \frac{1}{2} U \cos 2\alpha \cdot \sin 2\beta \right) \sin \delta_1 \cdot \sin \delta_2 \\
& + \frac{1}{2} V \cos 2\alpha \times \sin 2\beta \times \sin \delta_1 \times \cos \delta_2 \\
& + \frac{1}{2} V \sin 2\beta \times \cos \delta_1 \times \sin \delta_2 \\
& - \left( \frac{1}{4} Q \sin 4\alpha \cdot \sin 2\beta - \frac{1}{2} U \cos^2 2\alpha \cdot \sin 2\beta \right) \cdot \cos \delta_1 \cdot \cos \delta_2
\end{aligned}$$



# Dual PEM based method-the basic expansion

$$I' = \frac{1}{2}I + \frac{1}{2}Q \cos^2(2\alpha)\cos(2\beta) + \frac{1}{4}U \sin(4\alpha)\cos(2\beta) \quad 1-3$$

$$+ \frac{1}{2}\sin(2\alpha)\cos(2\beta)[Q \sin(2\alpha)-U \cos(2\alpha)]J_0(\delta_{10}) \quad 4$$

$$+ \frac{1}{2}\sin(2\alpha)\sin(2\beta)[Q \cos(2\alpha)+U \sin(2\alpha)]J_0(\delta_{20}) \quad 5$$

$$- \frac{1}{2}\cos(2\alpha)\sin(2\beta)[Q \sin(2\alpha)-U \cos(2\alpha)]J_0(\delta_{10})J_0(\delta_{20}) \quad 6$$

$$+ \{\sin(2\alpha)\sin(2\beta)[1-J_0(\delta_{10})][Q \cos(2\alpha)+U \sin(2\alpha)]+U \sin(2\beta)J_0(\delta_{10})\} \sum_n^\infty J_n(\delta_{20})\cos(n\Omega_2 t) \quad 7$$

$$+ [\sin(2\alpha)\cos(2\beta)-\cos(2\alpha)\sin(2\beta)J_0(\delta_{20})][Q \sin(2\alpha)-U \cos(2\alpha)] \sum_n^\infty J_n(\delta_{10})\cos(n\Omega_1 t) \quad 8$$

$$\mp \sin(2\beta)[Q \sin(2\alpha)-U \cos(2\alpha)] \sum_{m_1}^\infty \sum_{m_2}^\infty J_{m_1}(\delta_{10})J_{m_2}(\delta_{20})\cos[(m_1\Omega_1 \pm m_2\Omega_2)t] \quad 9$$

$$-\cos(2\alpha)\sin(2\beta)[Q \sin(2\alpha)-U \cos(2\alpha)] \sum_{n_1}^\infty \sum_{n_2}^\infty J_{n_1}(\delta_{10})J_{n_2}(\delta_{20})\cos[(n_1\Omega_1 \pm n_2\Omega_2)t] \quad 10$$

$$+ V \sin(2\beta)J_0(\delta_{10}) \sum_m^\infty J_m(\delta_{20})\sin(m\Omega_2 t) \quad 11$$

$$+ V [\cos(2\alpha)\sin(2\beta)J_0(\delta_{20})-\sin(2\alpha)\cos(2\beta)] \sum_m^\infty J_m(\delta_{10})\sin(m\Omega_1 t) \quad 12$$

$$+ V \cos(2\alpha)\sin(2\beta) \sum_m^\infty \sum_n^\infty J_m(\delta_{10})J_n(\delta_{20})\sin[(m\Omega_1 \pm n\Omega_2)t] \quad 13$$

$$\pm V \sin(2\beta) \sum_n^\infty \sum_m^\infty J_n(\delta_{10})J_m(\delta_{20})\sin[(n\Omega_1 \pm m\Omega_2)t] \quad 14$$



TABLE I. Frequencies of signals required to determine the Stokes parameters for different sets of angular variables.

Case	Condition	<i>I</i>	<i>Q</i>	<i>U</i>	<i>V</i>
I	$\alpha=45^\circ$ , $\beta=\text{arbitrary}$ [ $\sin(2\beta) \neq 0$ ]	dc	$2\Omega_1[\cos(2\beta) \neq 0]$ or $\Omega_1 \pm \Omega_2$	$2\Omega_2$	$\Omega_1[\cos(2\beta) \neq 0]$ or $2\Omega_1 \pm \Omega_2$
II	$\beta=45^\circ$ , $\alpha=\text{arbitrary}$ [ $\sin(2\alpha) \neq 0$ ]	dc	$2\Omega_2$ and $2\Omega_1 \pm 2\Omega_2$ [ $\cos(2\alpha) \neq 0$ ] or $2\Omega_2$ and $\Omega_1 \pm \Omega_2$	$\Omega_1 \pm 2\Omega_2$ [ $\cos(2\alpha) \neq 0$ ] or $2\Omega_1 \pm \Omega_2$	
III	$\alpha=\text{arbitrary}$ $\beta=\text{arbitrary}$ [ $\sin(2\beta) \neq 0$ and $\sin(2\alpha) \neq 0$ ]	dc with <i>Q</i> and <i>U</i>	$2\Omega_1$ and $2\Omega_2$ [ $\cos(2\beta) \neq 0$ ] or $2\Omega_2$ and $\Omega_1 \pm \Omega_2$ or $2\Omega_2$ and $2\Omega_1 \pm \Omega_2$ [ $\cos(2\alpha) \neq 0$ ]	$\Omega_1 \pm 2\Omega_2$ [ $\cos(2\alpha) \neq 0$ ] or $\Omega_1[\cos(2\beta) \neq 0]$ or $2\Omega_1 \pm \Omega_2$	



TABLE II. Frequencies of signals required to determine the Stokes parameters in special cases where both angular variables are specified.

Case	$\alpha$ (deg)	$\beta$ (deg)	$I$	$Q$	$U$	$V$
a	45	22.5	dc	$2\Omega_1$	$2\Omega_2$	$\Omega_1$
b	45	45	dc	$\Omega_1 \pm \Omega_2$	$2\Omega_2$	$2\Omega_1 \pm \Omega_2$
c	22.5	45	dc	$2\Omega_2$ and $2\Omega_1 \pm 2\Omega_2$		$2\Omega_1 \pm \Omega_2$

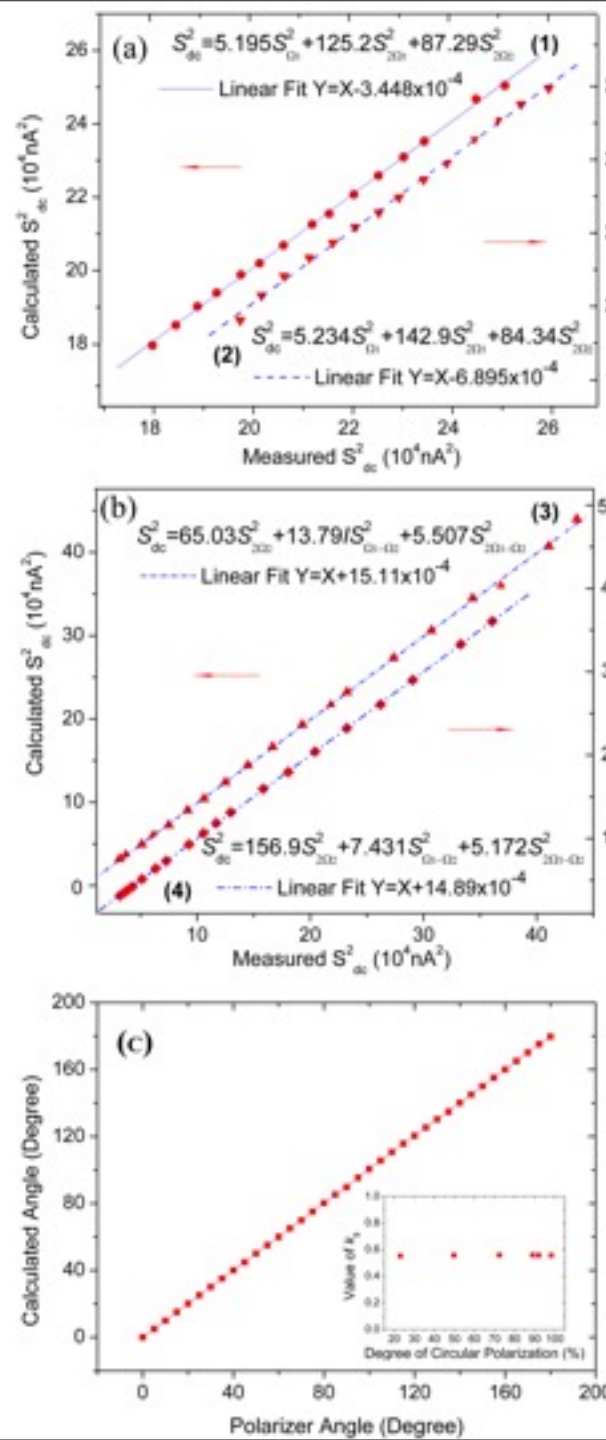


# calibration

Liu et al. JAP (2006)

For purely polarised light,

$$I^2 = Q^2 + U^2 + V^2$$



# calibration matrix

$$I_{dc} = c_1 I + c_2 Q + c_3 U$$

$$I_{QU1} = c_4 Q + c_5 U$$

$$S_{dc} = v_1 I_{dc} = g_1 I + g_2 Q + g_3 U$$

$$I_{QU2} = c_6 Q + c_7 U$$

$$S_{QU1} = v_2 I_{QU1} = g_4 Q + g_5 U$$

$$I_V = c_8 V$$

$$S_{QU2} = v_3 I_{QU2} = g_6 Q + g_7 U$$

$$S_V = v_4 I_V = g_8 V$$



# calibration matrix

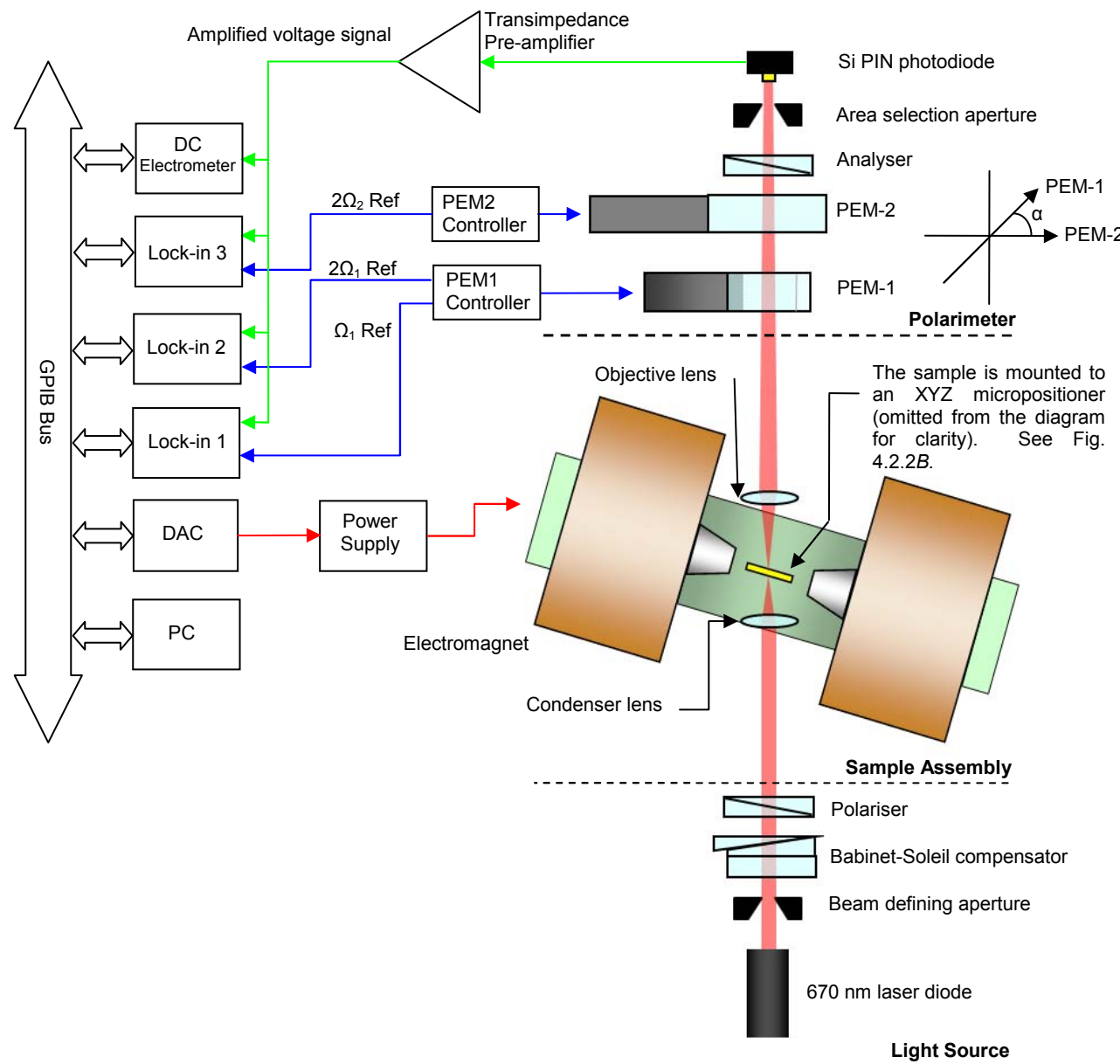
$$\begin{pmatrix} S_{dc} \\ S_{QU1} \\ S_{QU2} \\ S_V \end{pmatrix} = \begin{pmatrix} g_1 & g_2 & g_3 & 0 \\ 0 & g_4 & g_5 & 0 \\ 0 & g_6 & g_7 & 0 \\ 0 & 0 & 0 & g_8 \end{pmatrix} \begin{pmatrix} I \\ Q \\ U \\ V \end{pmatrix} = G \begin{pmatrix} I \\ Q \\ U \\ V \end{pmatrix}$$

$$\begin{pmatrix} I \\ Q \\ U \\ V \end{pmatrix} = \begin{pmatrix} k_1 & k_2 & k_3 & 0 \\ 0 & k_4 & k_5 & 0 \\ 0 & k_6 & k_7 & 0 \\ 0 & 0 & 0 & k_8 \end{pmatrix} \begin{pmatrix} S_{dc} \\ S_{QU1} \\ S_{QU2} \\ S_V \end{pmatrix} = K \begin{pmatrix} S_{dc} \\ S_{QU1} \\ S_{QU2} \\ S_V \end{pmatrix}$$

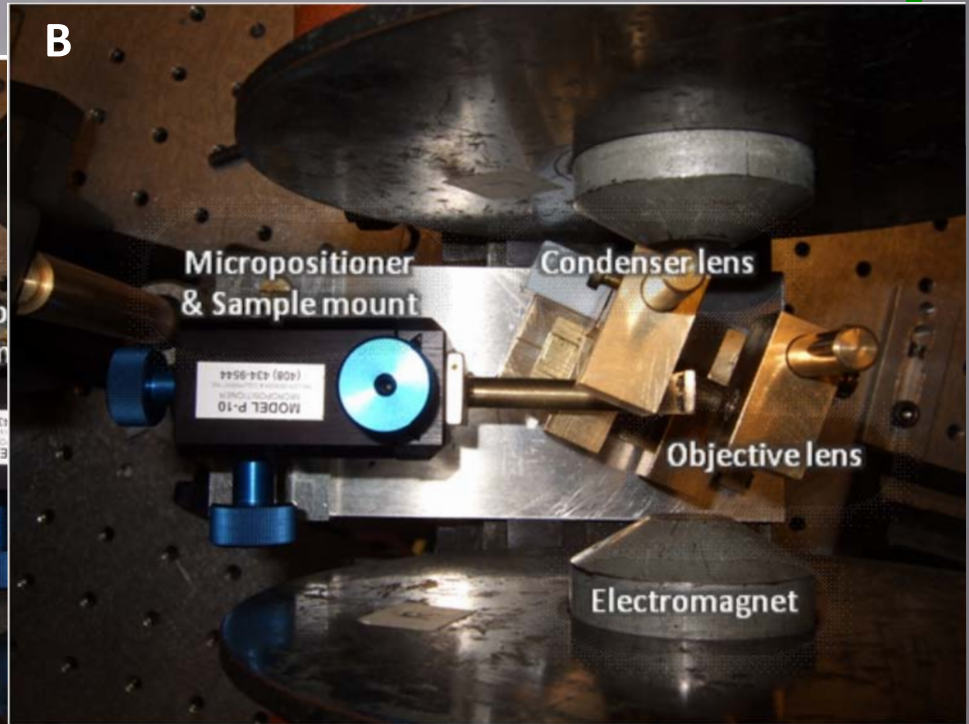
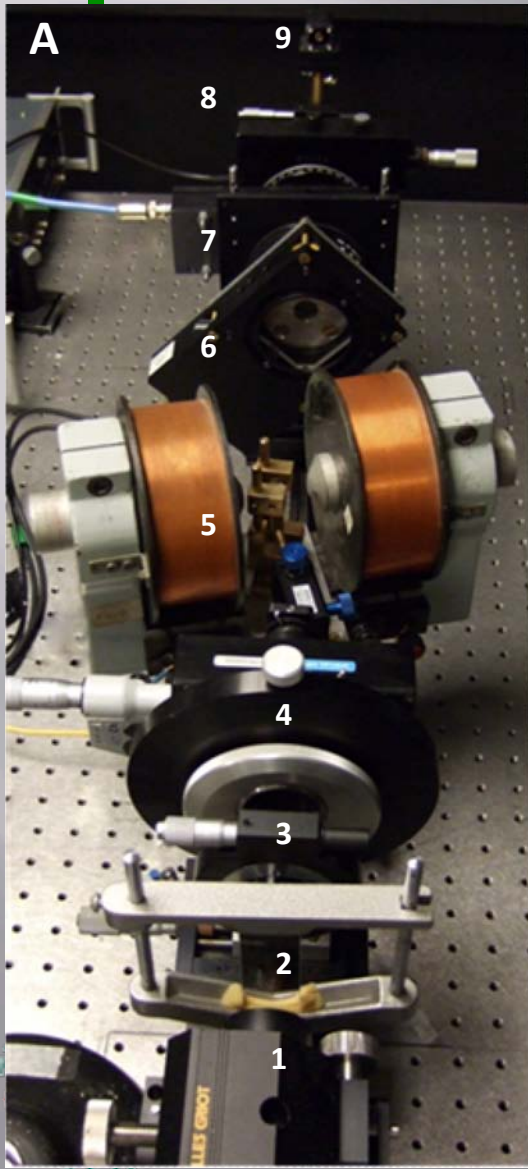
$K$  is a set of constants that are specific to the experimental setup and determined through a calibration procedure.



# A practical magneto optical Stokes polarimeter



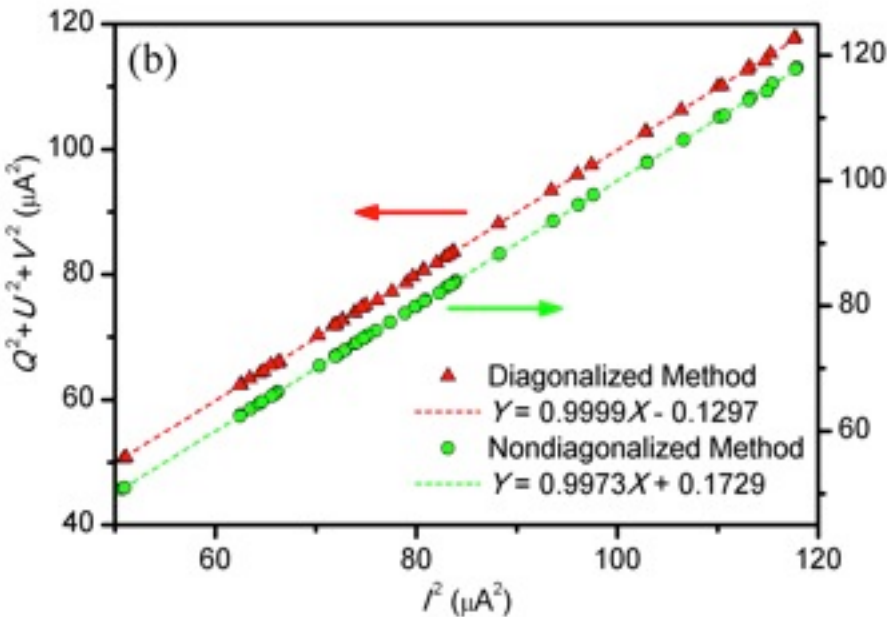
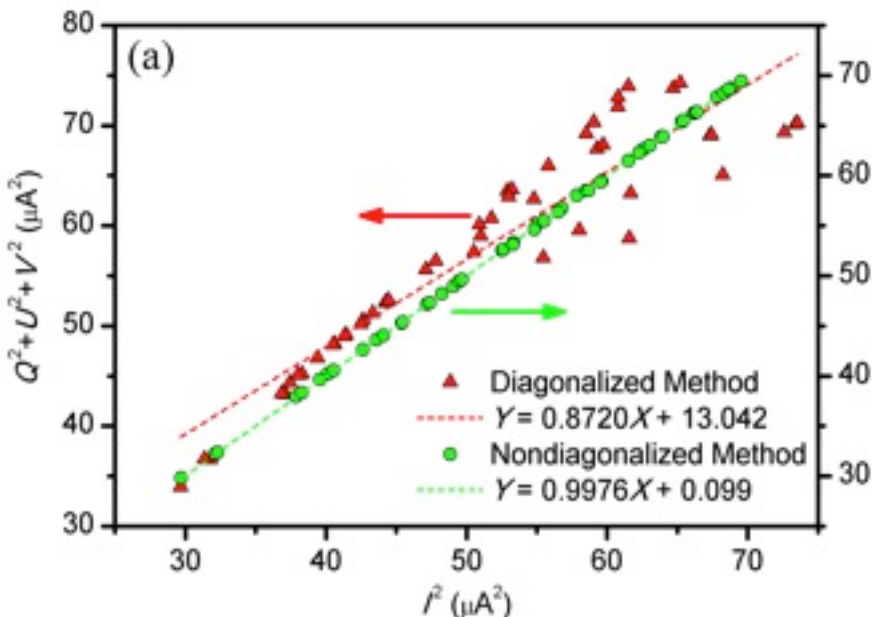
# A practical magneto optical Stokes polarimeter



(A): A photograph of the polarimeter. The components visible are the: (1) laser, (2) neutral density filter, (3) polariser, (4) Babinet-Soleil compensator, (5) electromagnet/sample mount and lenses, (6) PEM-1, PEM2, (8) analysing polariser (hidden behind 7) and (9) Si-PIN photodiode. (B): A close-up photograph of the sample mount and lens assembly.

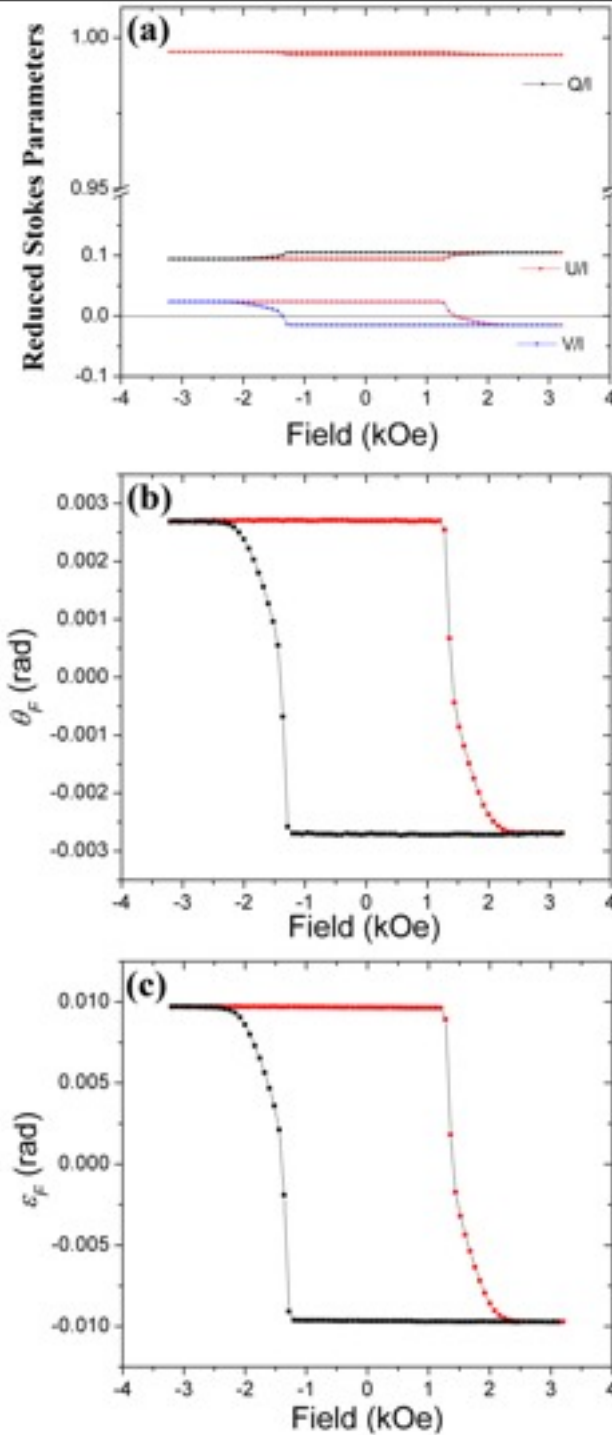
# Robustness

Guan et al.  
Appl. Opt. (2010)



## Example -Faraday effect in CoPt multilayers

15 bilayers of  
Co0.4nm/Pt1.0nm



# NANOSTRUCTURED MATERIALS

-A study of the magneto  
optical characteristics



# the motivations of our own work

- the responses of nanostructured materials to the polarisation states of incident radiation
- the magneto optical characteristics of magnetic nanostructures
- the interaction of (circularly) polarised light with electron spin states (spin polarised electron injection)



# NANOSTRUCTURED MATERIALS

-A study of the magneto optical  
characteristics of anodic  
aluminium oxide (AAO)



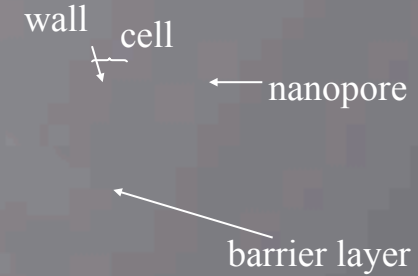
**Preparation and characterisation of anodic aluminium oxide (AAO) and the nanowire arrays**

**Magneto-optical properties of Fe nanowire arrays**

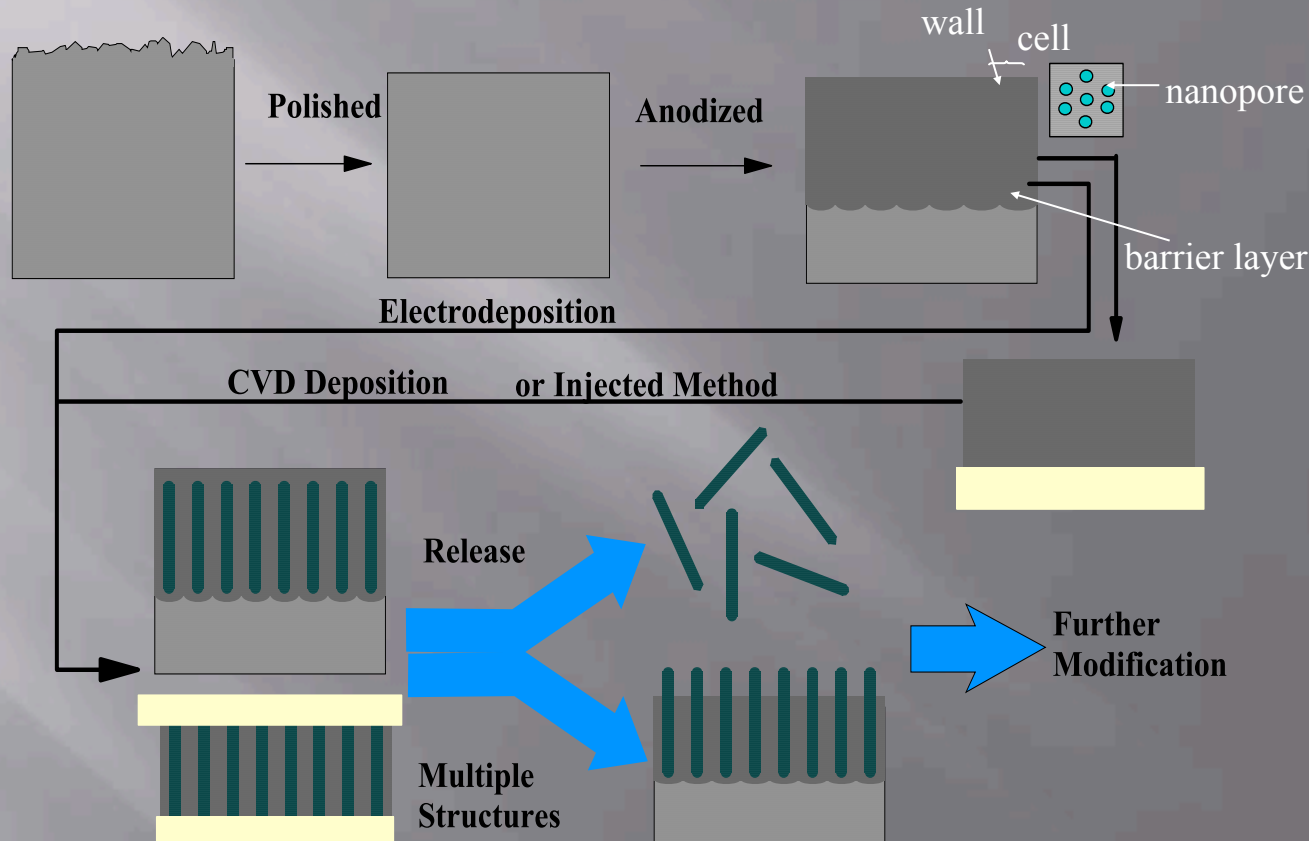
**Magneto-optical properties of Co nanowire arrays**



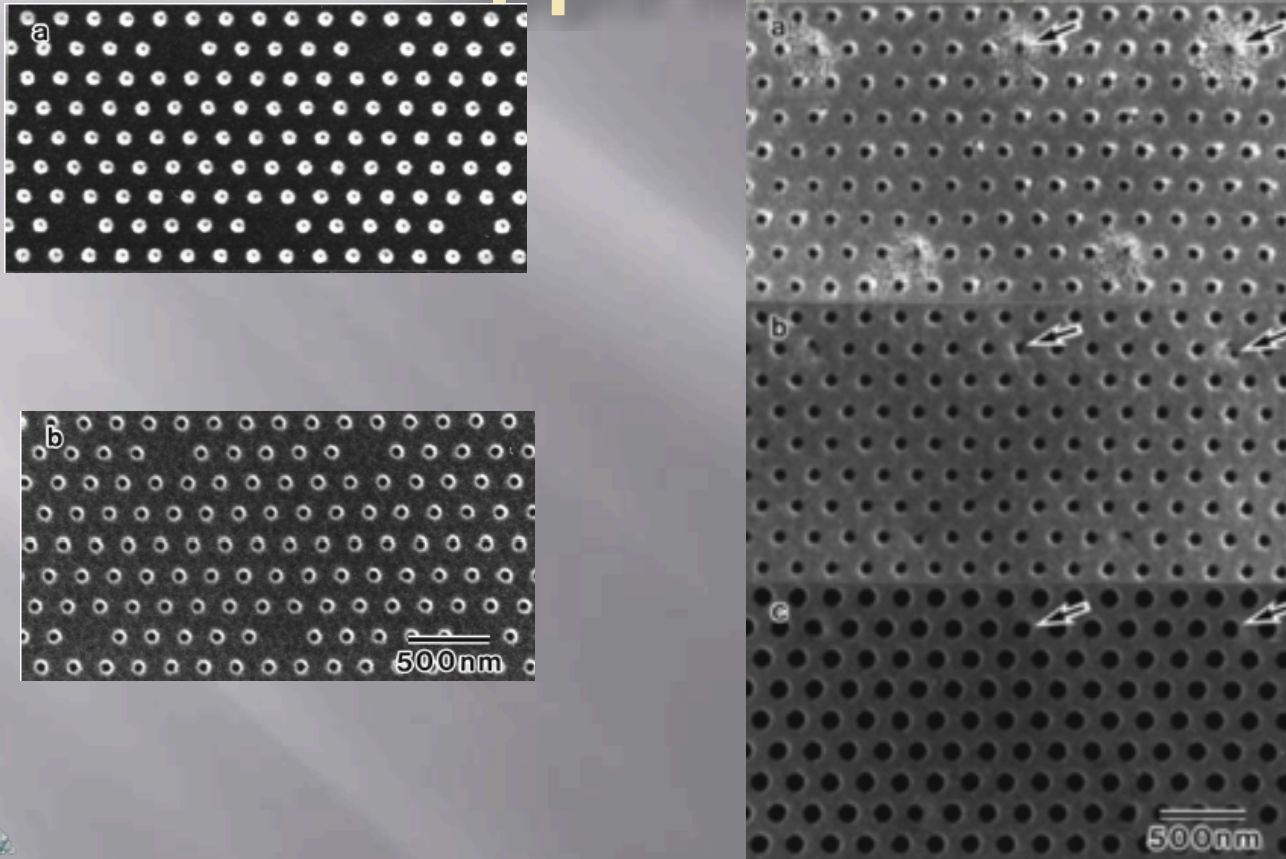
# AAO Template method-sample preparation



# AAO Template method-sample preparation



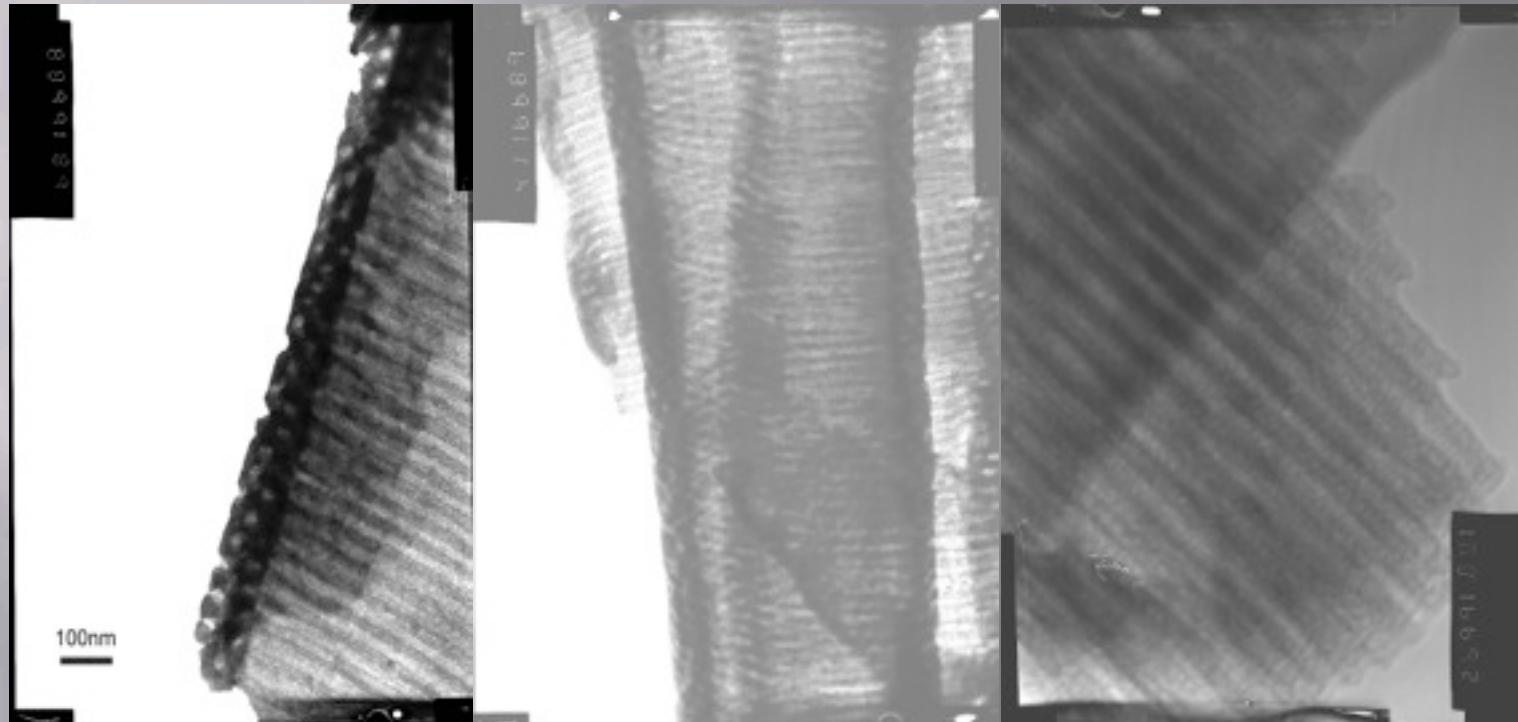
# Self-organised growth/self repair of defect structure (Masuda, et al, App.Phv.Lett.)





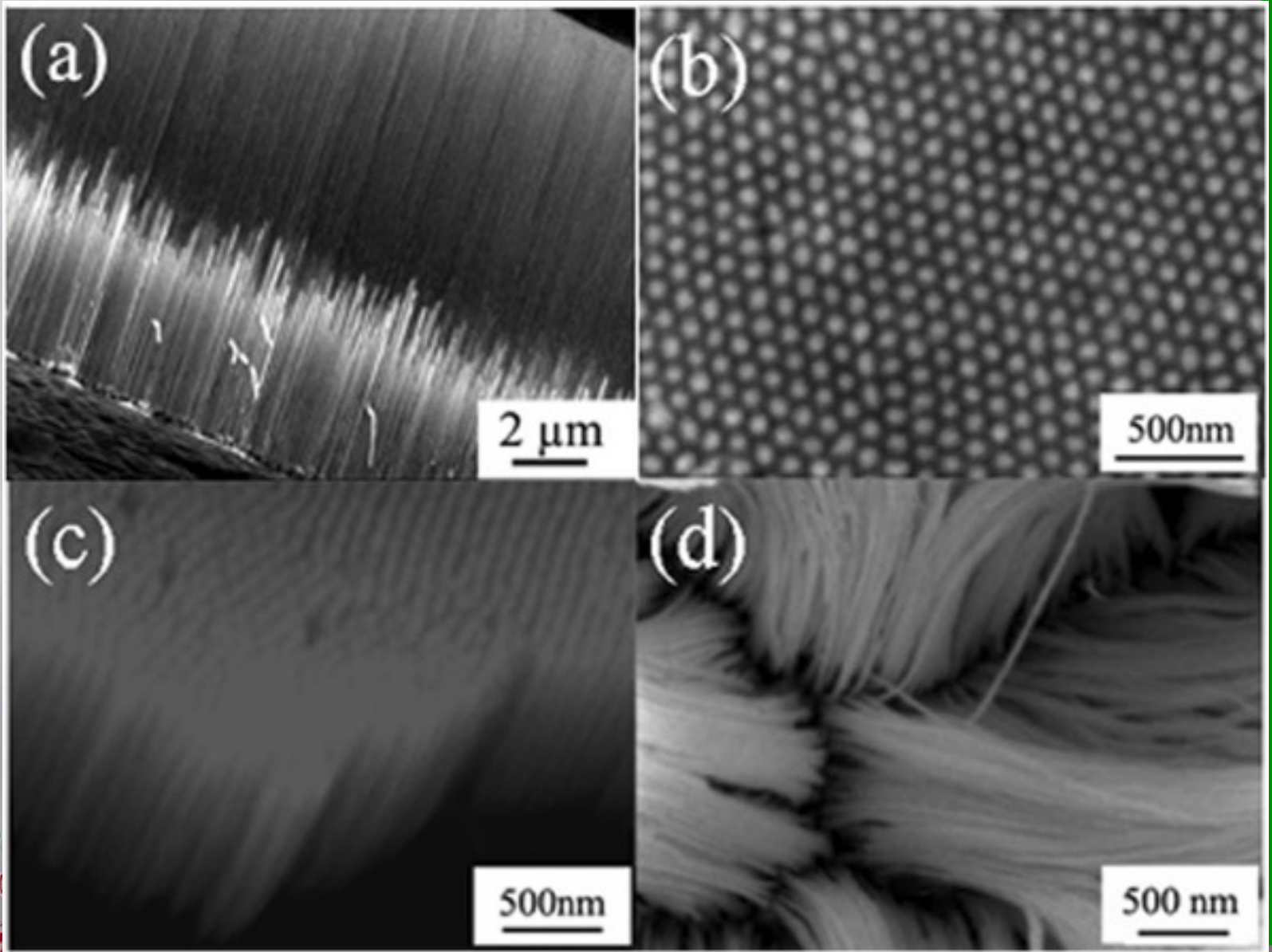
# Characterisation-

## TEM Images of Fe-nanowire embedded in AAO template



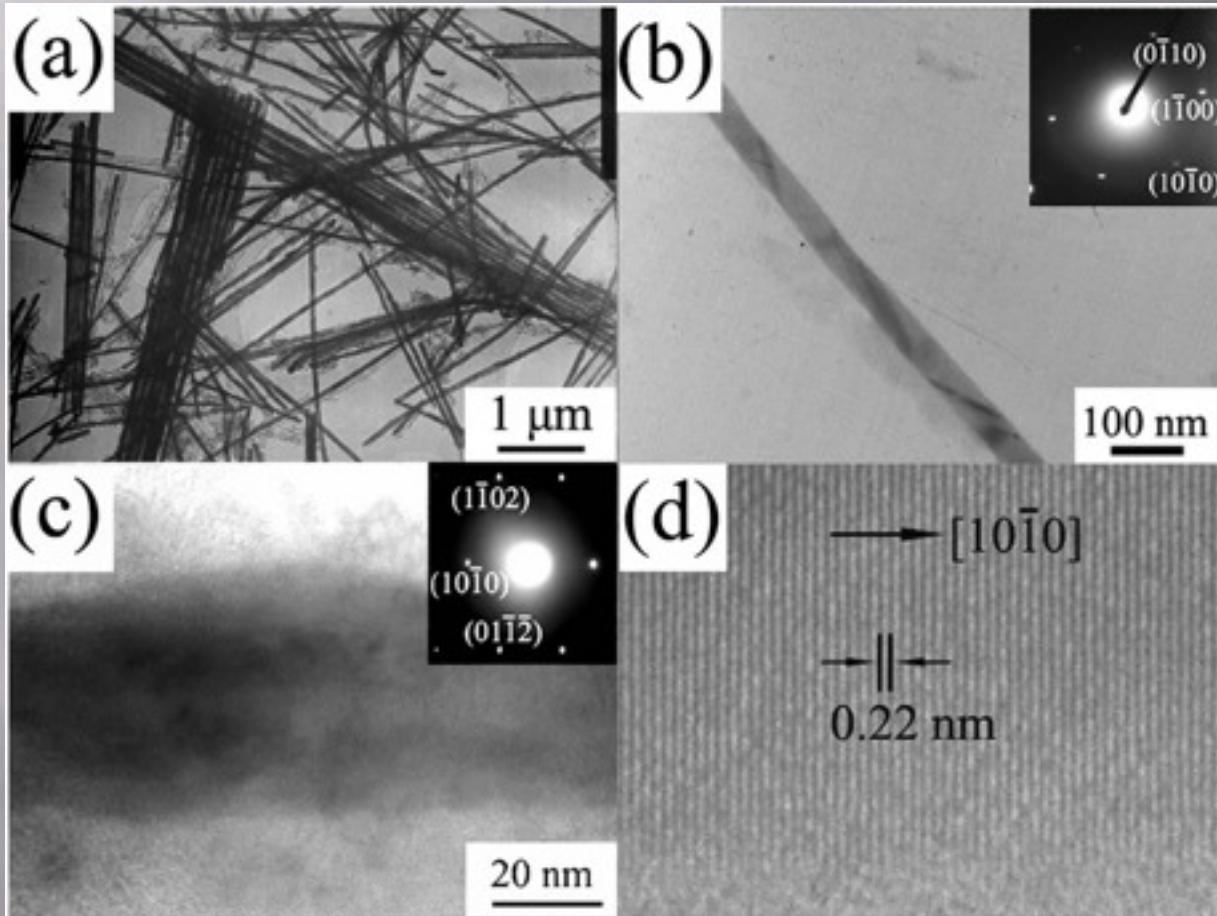
$d \approx 15\text{nm}$



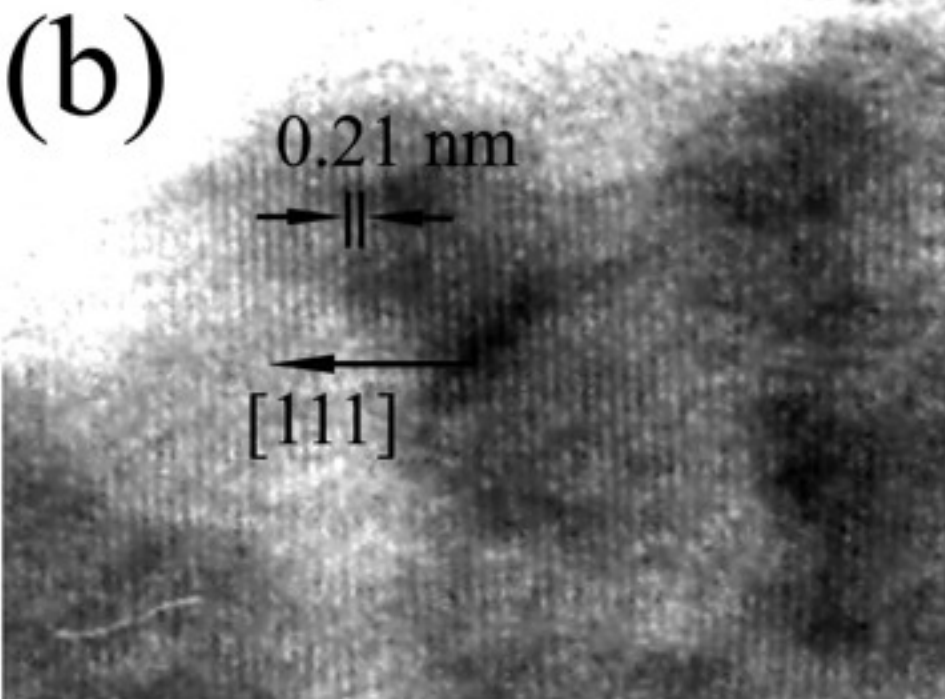
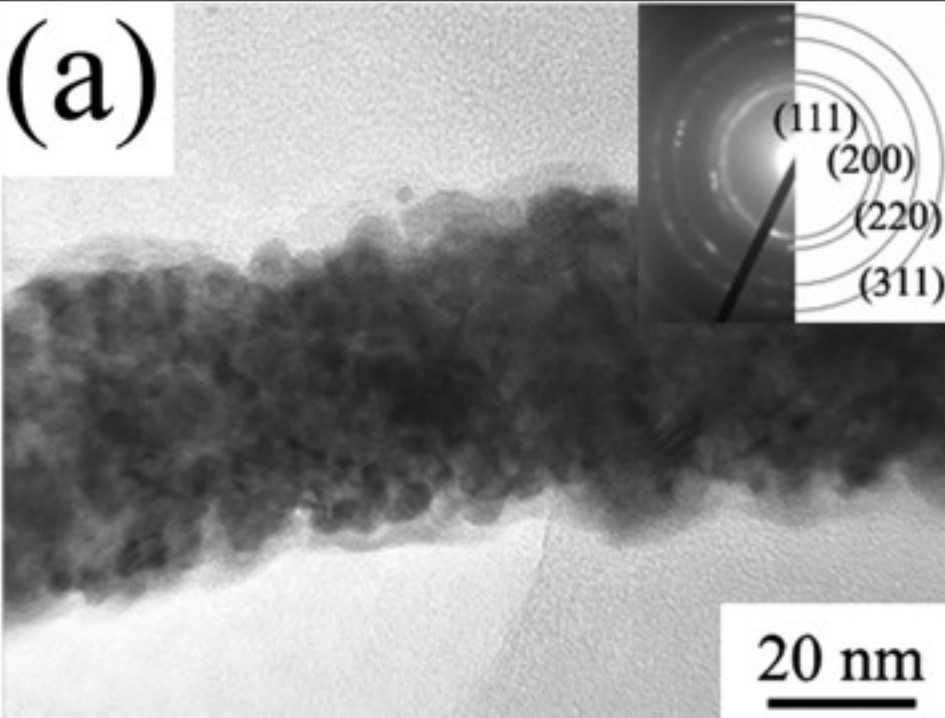


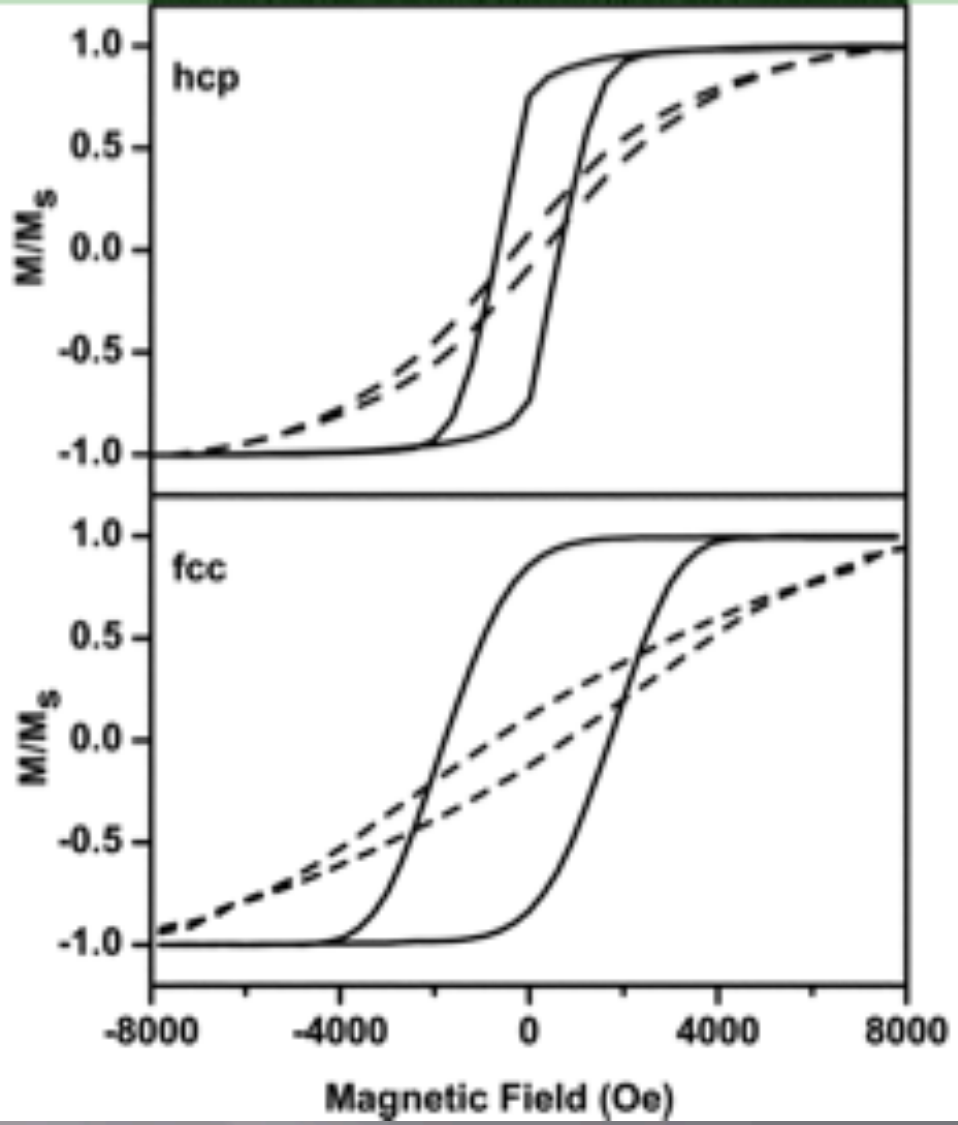
# hcp Co

Zhang, et al. JAP (2007)



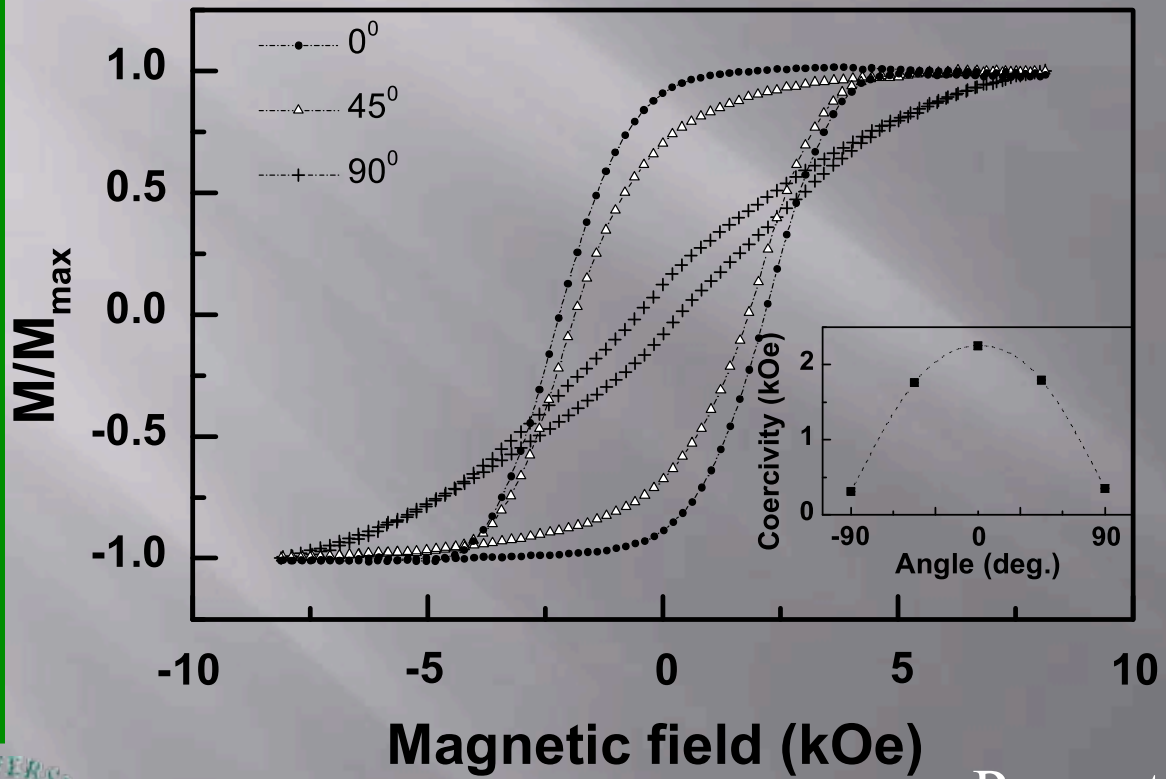
Fcc Co





# Characterisation-

## Magnetic properties of nano-wire arrays in AAO (VSM)

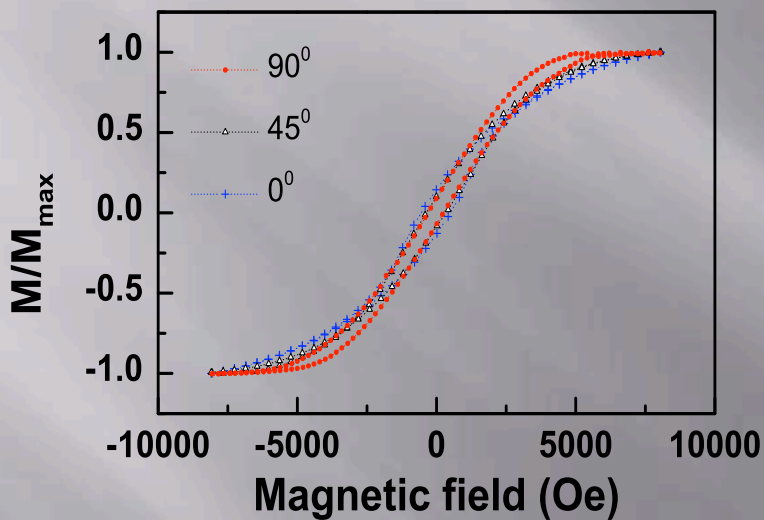


Peng et al. APL (2003)

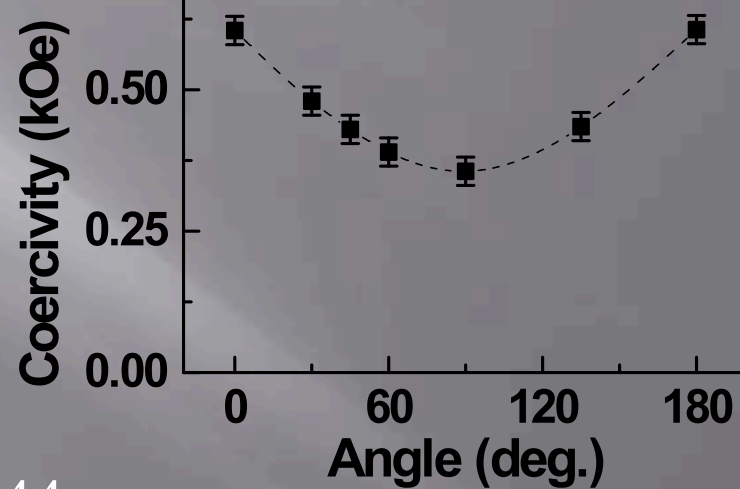


# Characterisation-

## Magnetic properties of nano-wire arrays in AAO (VSM)

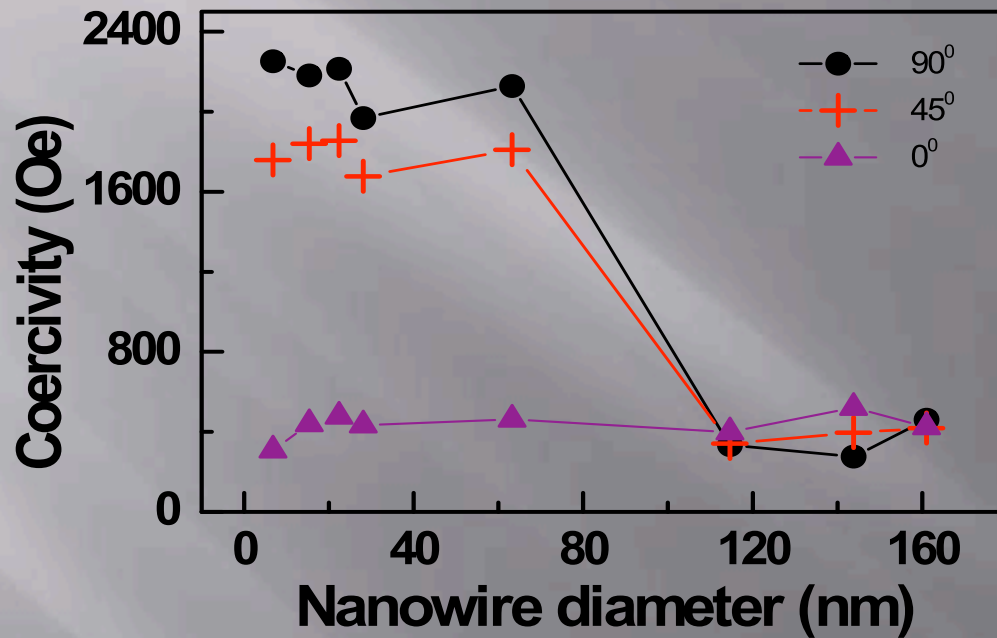


$d=144 \text{ nm}$

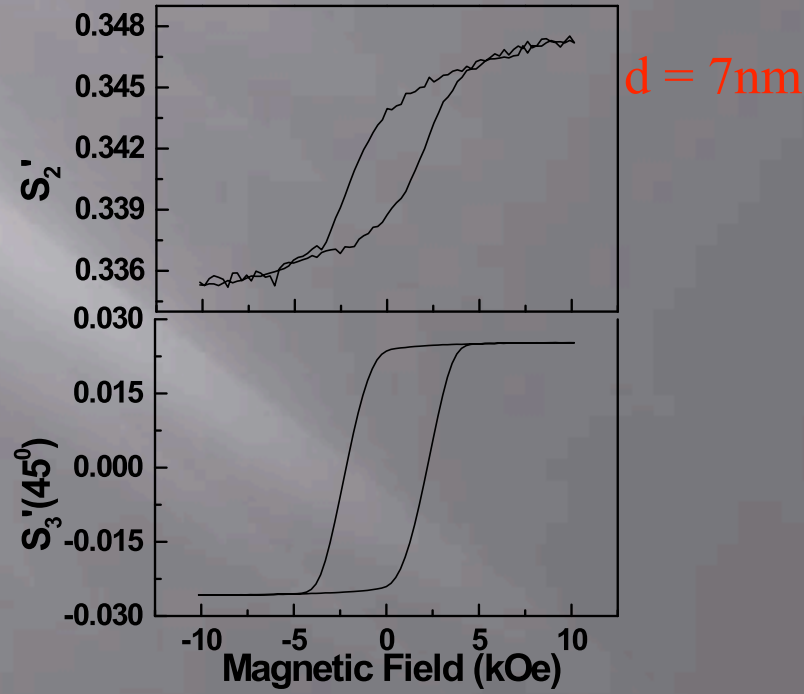
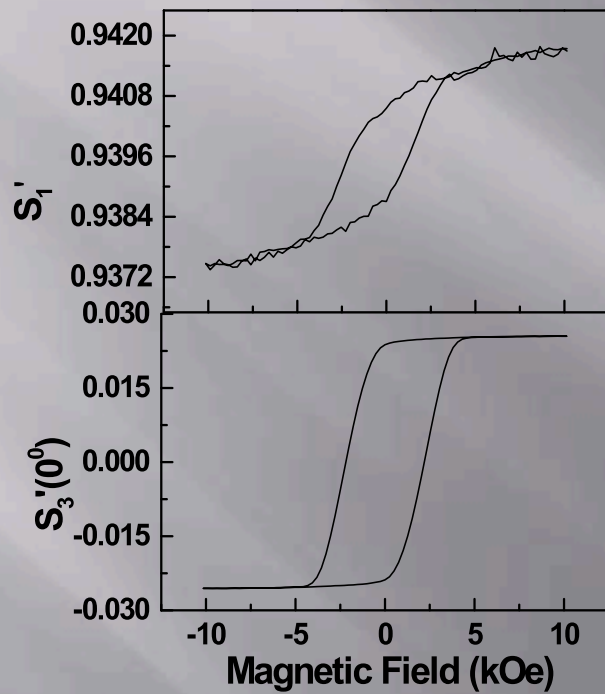


## Characterisation-

# Magnetic properties of nano-wire arrays in AAO (VSM)



# Results – MO properties of Fe nanowire array in AAO matrix

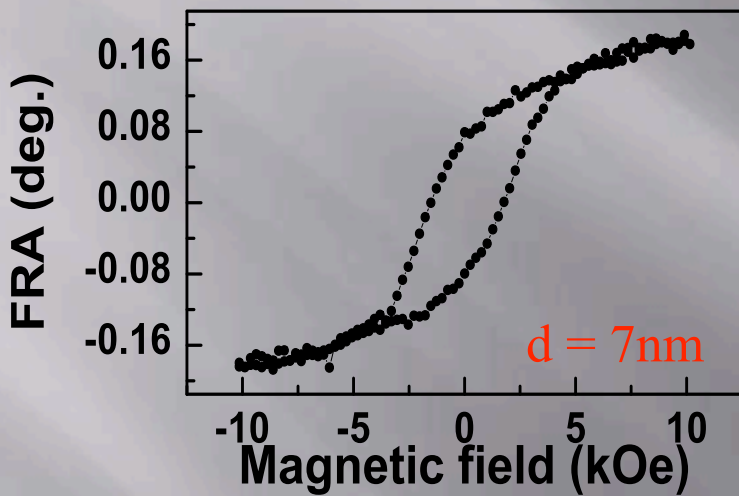


normalized Stokes parameters of a 7nm diameter Fe nanowire array

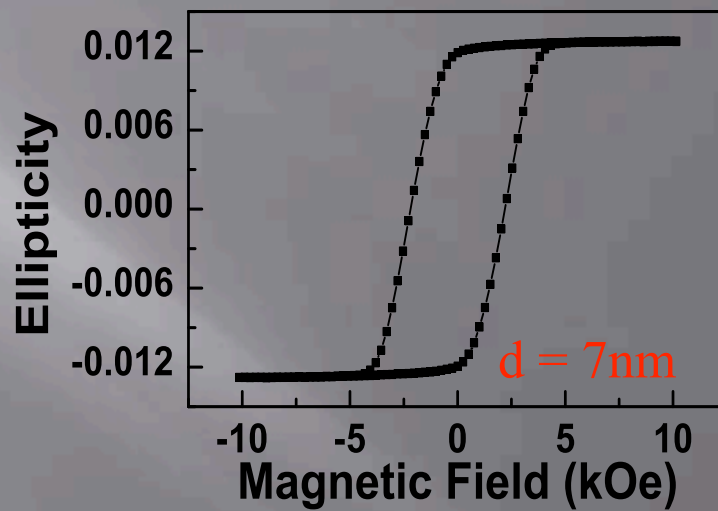


## Results-

### MO properties of Fe nanowire array in AAO matrix



Max. FRA: 0.184

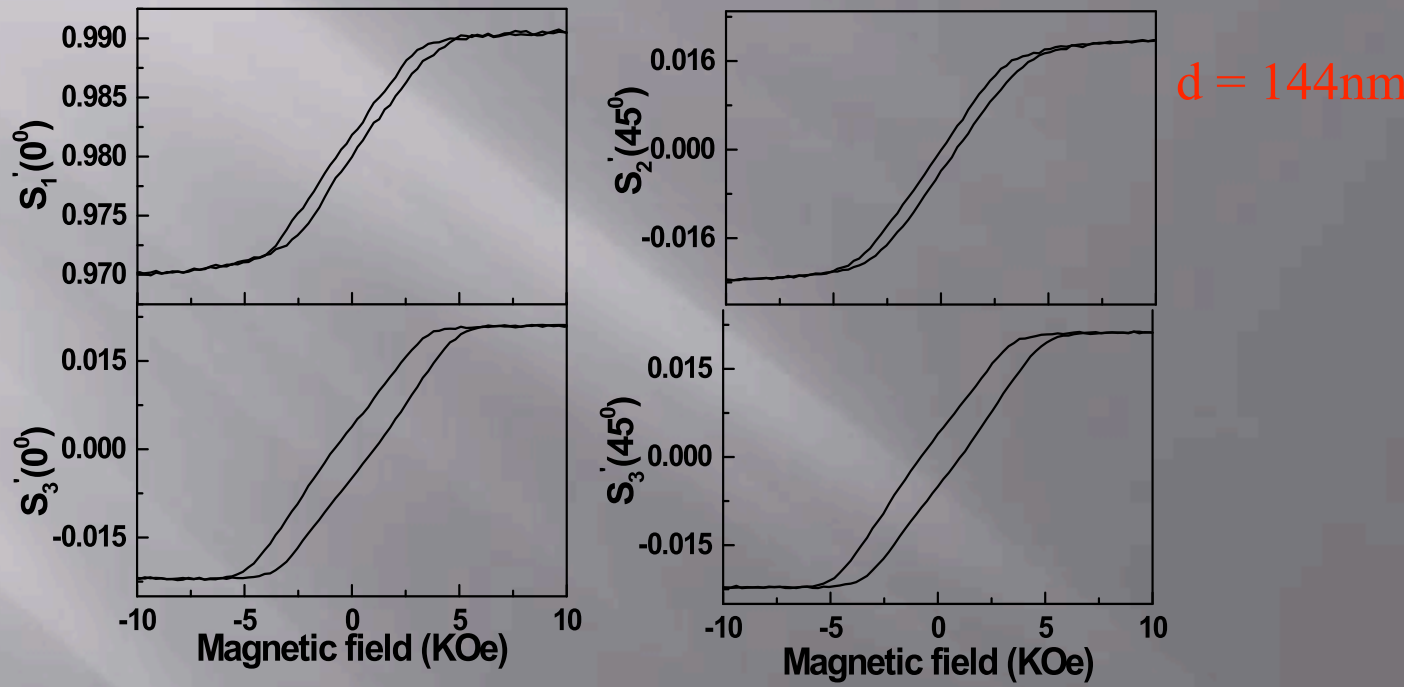


Max. Ellipticity ( $\tan\chi$ ): 0.0127

FRA and ellipticity vs magnetic field for a 7nm nanowire array



# Results – MO properties of Fe nanowire array in AAO matrix

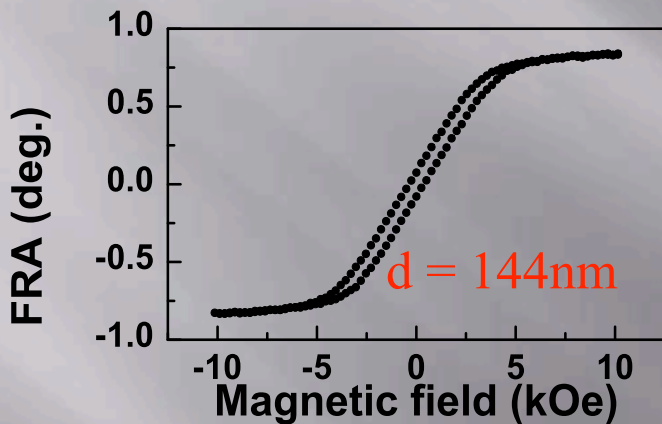


normalized Stokes parameters of a 144nm diameter Fe nanowire array

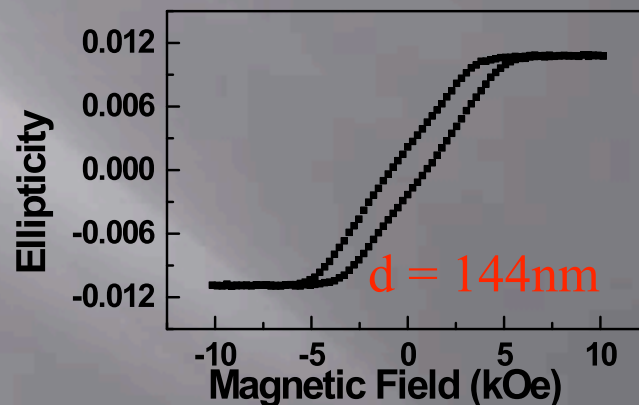


## Results-

# MO properties of Fe nanowire array in AAO matrix



Max. FRA:  $0.830^0$



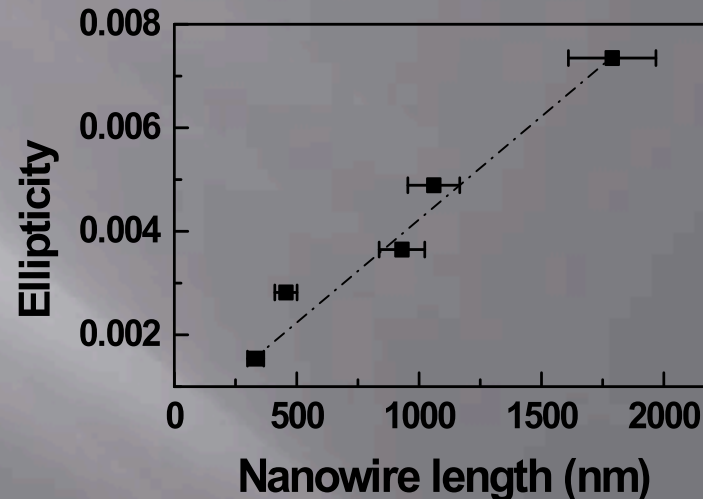
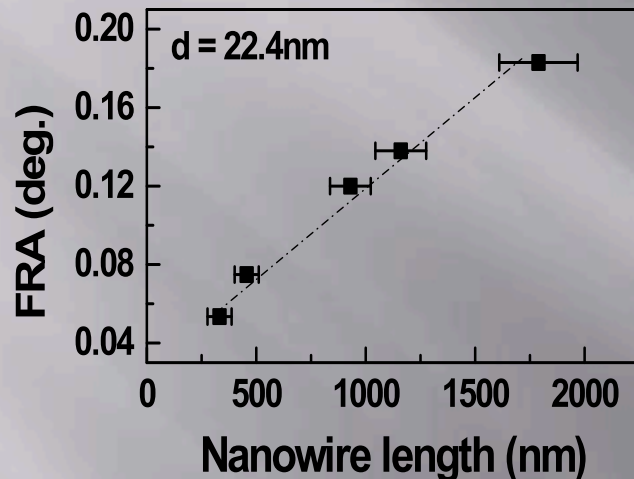
Max. Ellipticity ( $\tan\chi$ ):  $0.0108$

FRA and ellipticity vs magnetic field for a 144nm nanowire array



## Results-

### MO properties of Fe nanowire array in AAO matrix



FRA is linear with nanowire length;

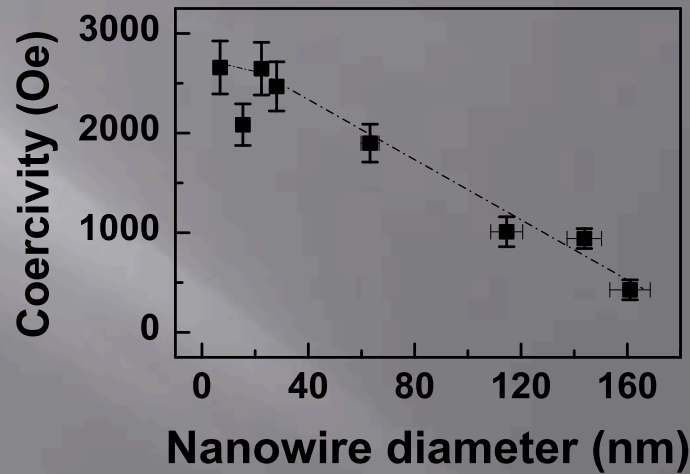
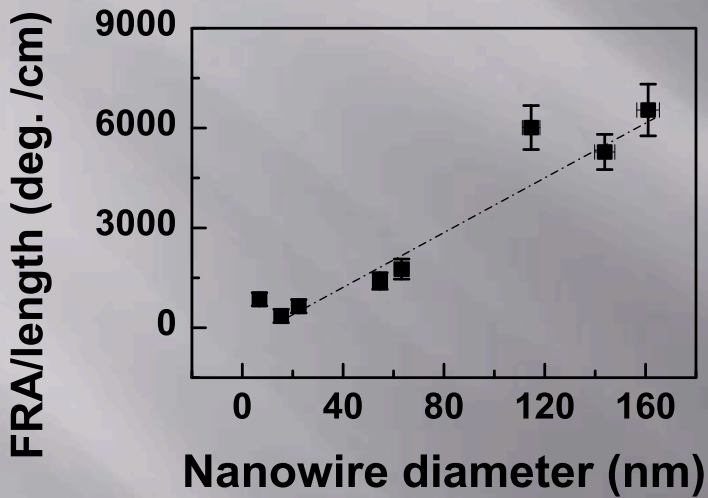
Let  $\theta = VHL$ ,  $V = 0.0081 \text{ deg}\cdot\text{cm}^{-1}\cdot\text{Oe}^{-1}$ , far less than bulk Fe;

Ellipticity vs nanowire length appeared to be linear.

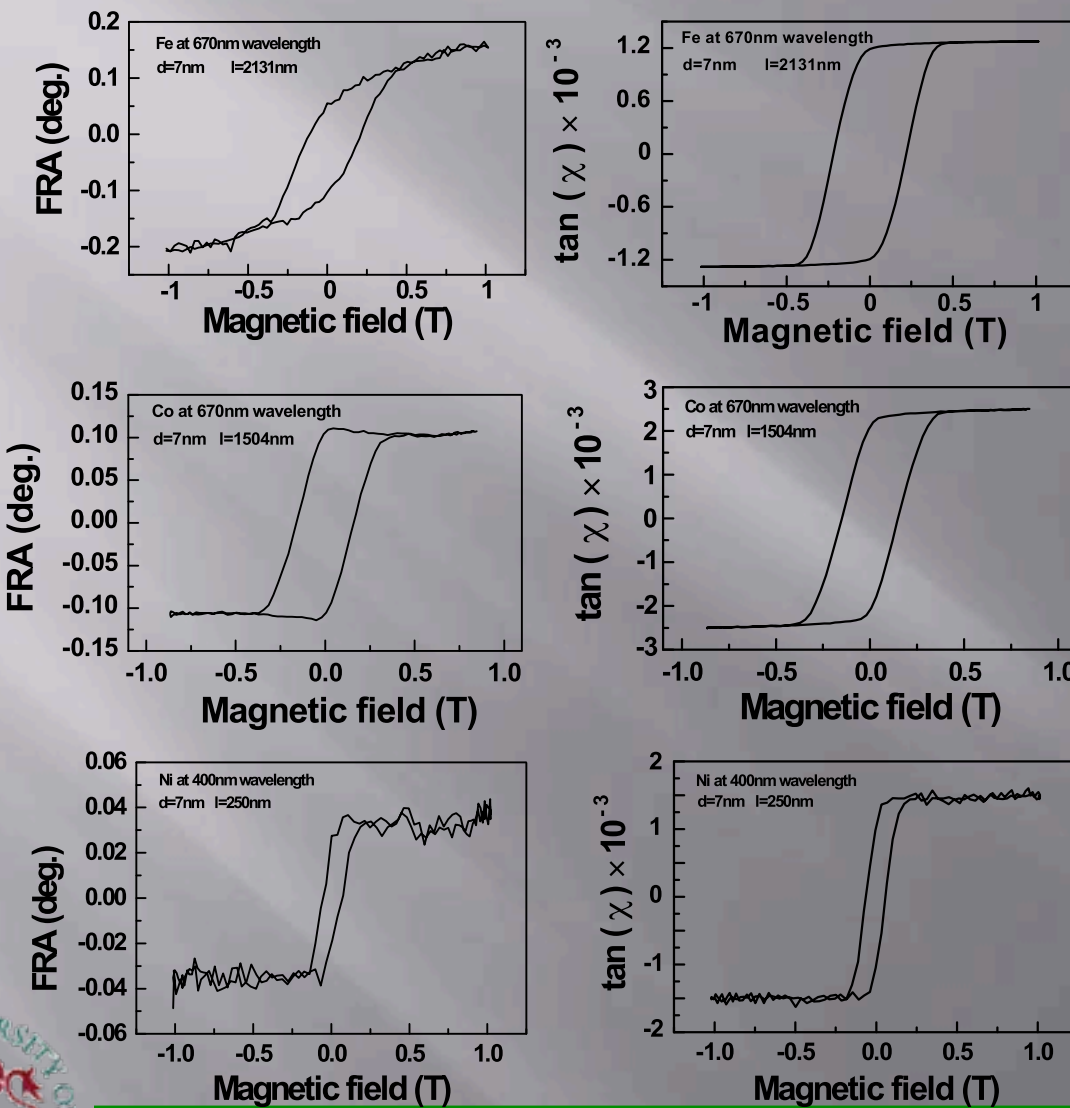


## Results-

### MO properties of Fe nanowire array in AAO matrix



A comparison of Fe, Co and Ni nanowire arrays with wire diameter of 7nm.



# key experimental observations

- Magneto optical effects are much smaller in nanowire arrays compared with their bulk counterparts
- The details of nano scale structures do influence the magneto optical characteristics
- No observable depolarisation by nano structures has been found.



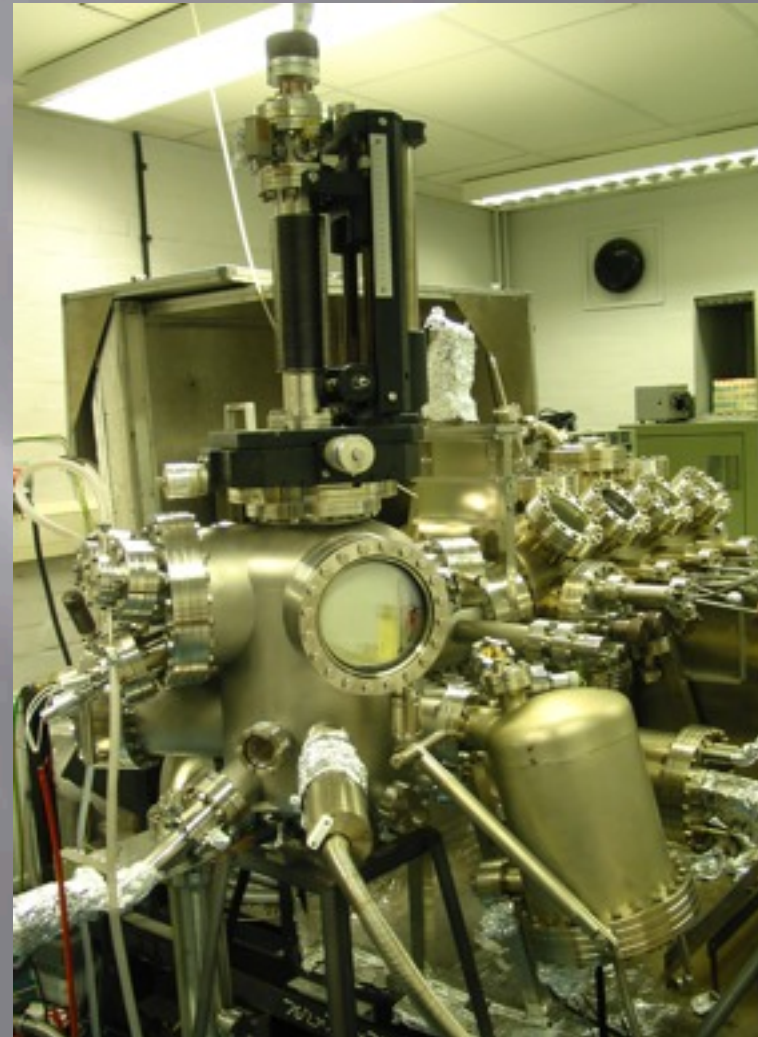
# NANOSTRUCTURED MATERIALS

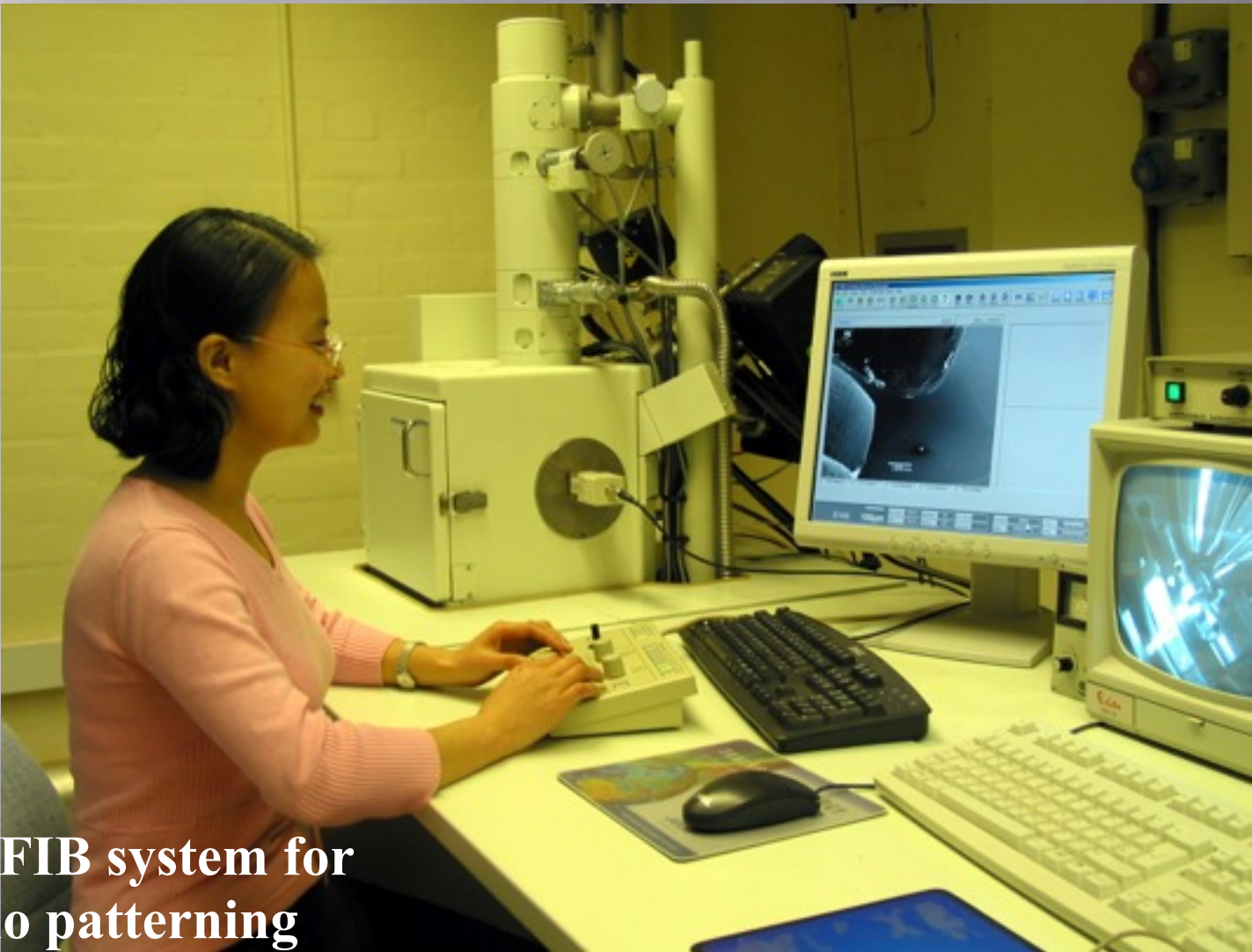
-nano structured patterned films



## Sample preparation: -thin film

### UHV e-beam deposition

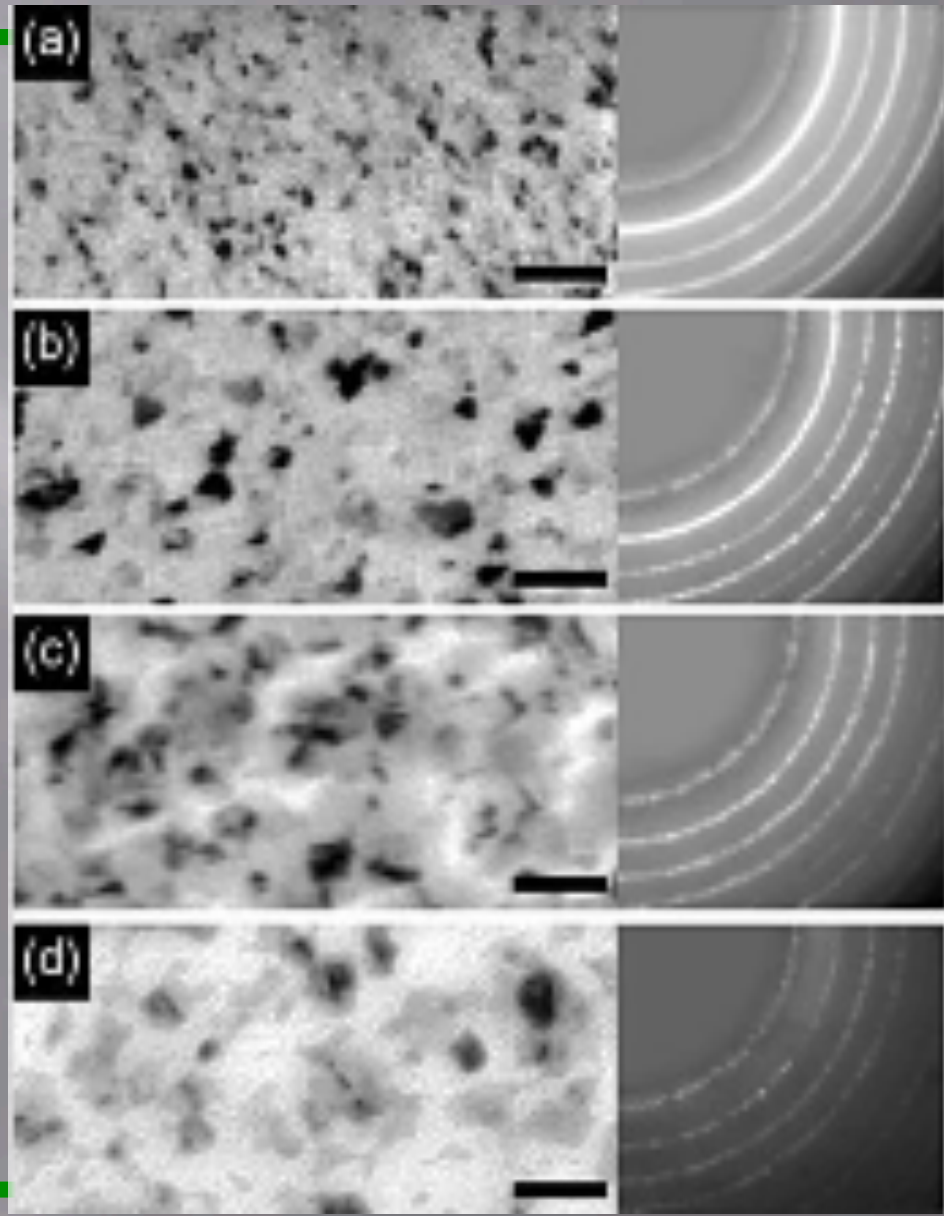




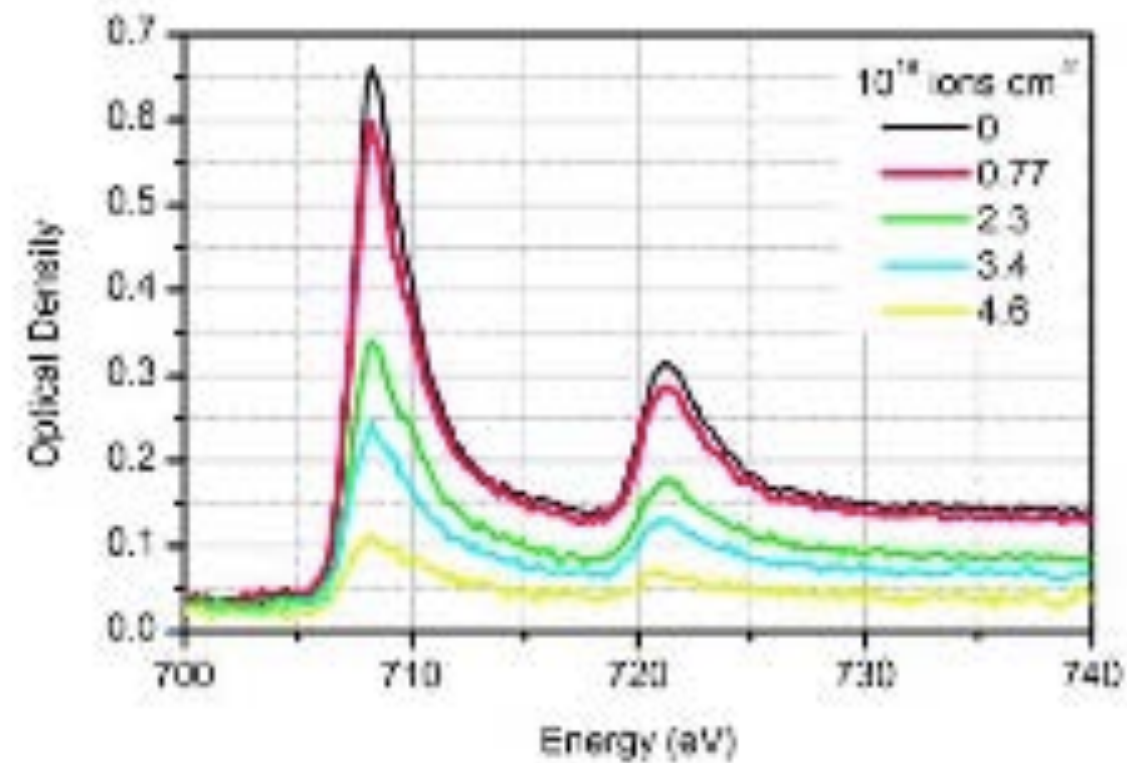
An FIB system for  
nano patterning



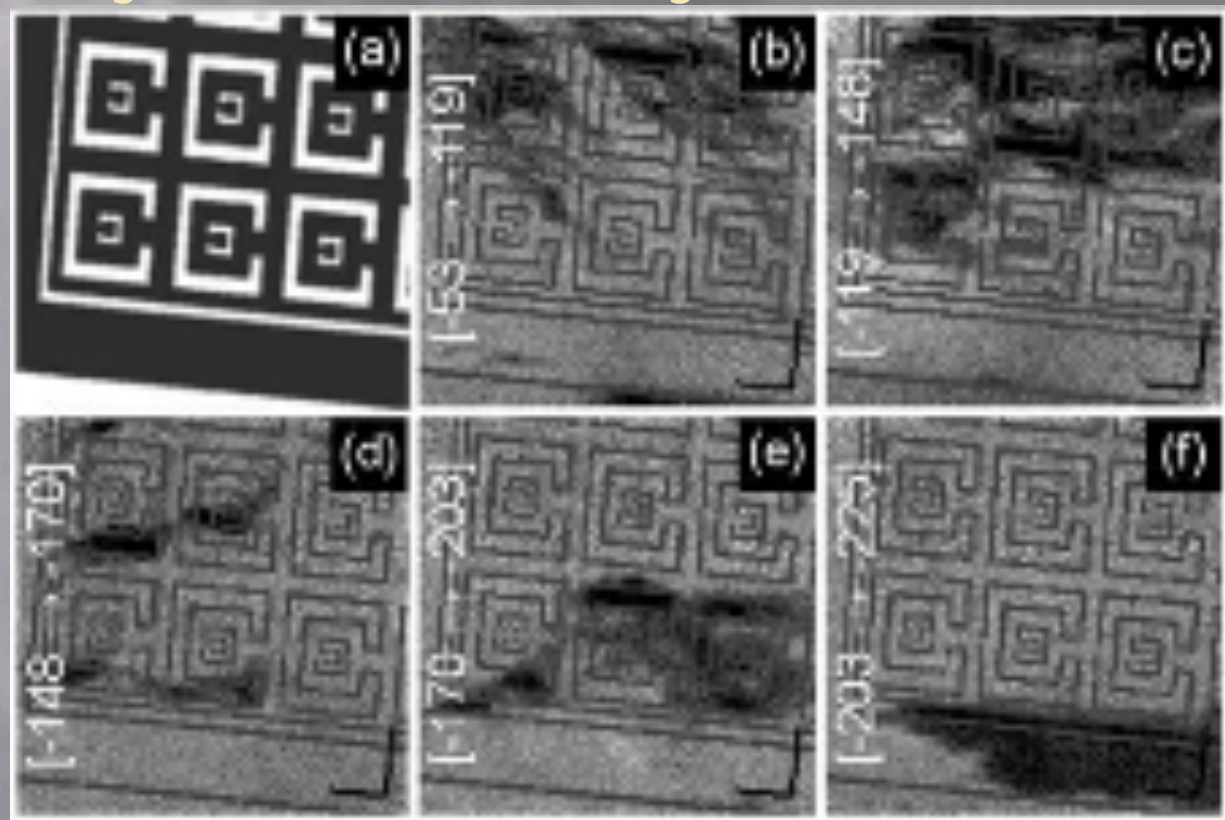
TEM images and SAED patterns for the as-grown Fe (a) and the Fe-Ga irradiated with (b)  $7.7 \times 10^{15}$ , (c)  $2.3 \times 10^{16}$  and (d)  $3.4 \times 10^{16}$  ions  $\text{cm}^{-2}$ . The scale bars represent 100 nm.



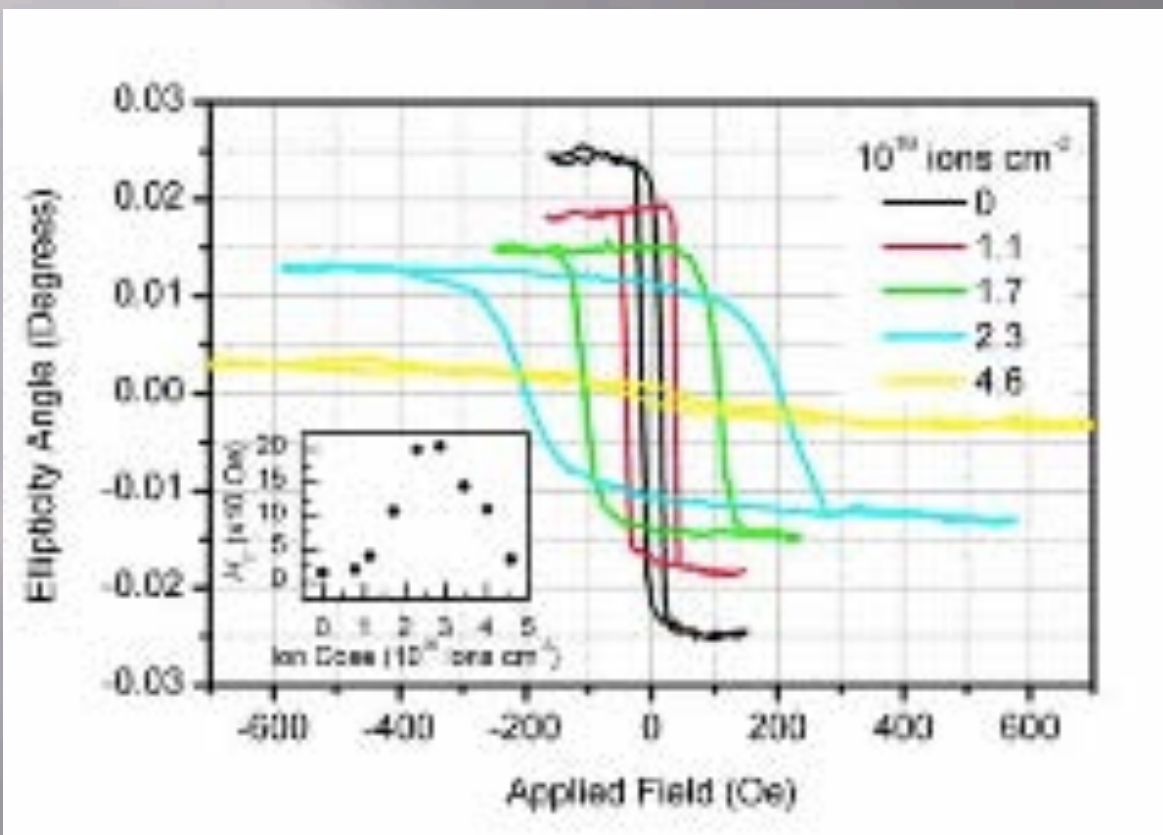
XAS showing the Fe L<sub>2,3</sub> absorption peaks at 721 and 708 eV respectively for the as- grown and irradiated film.



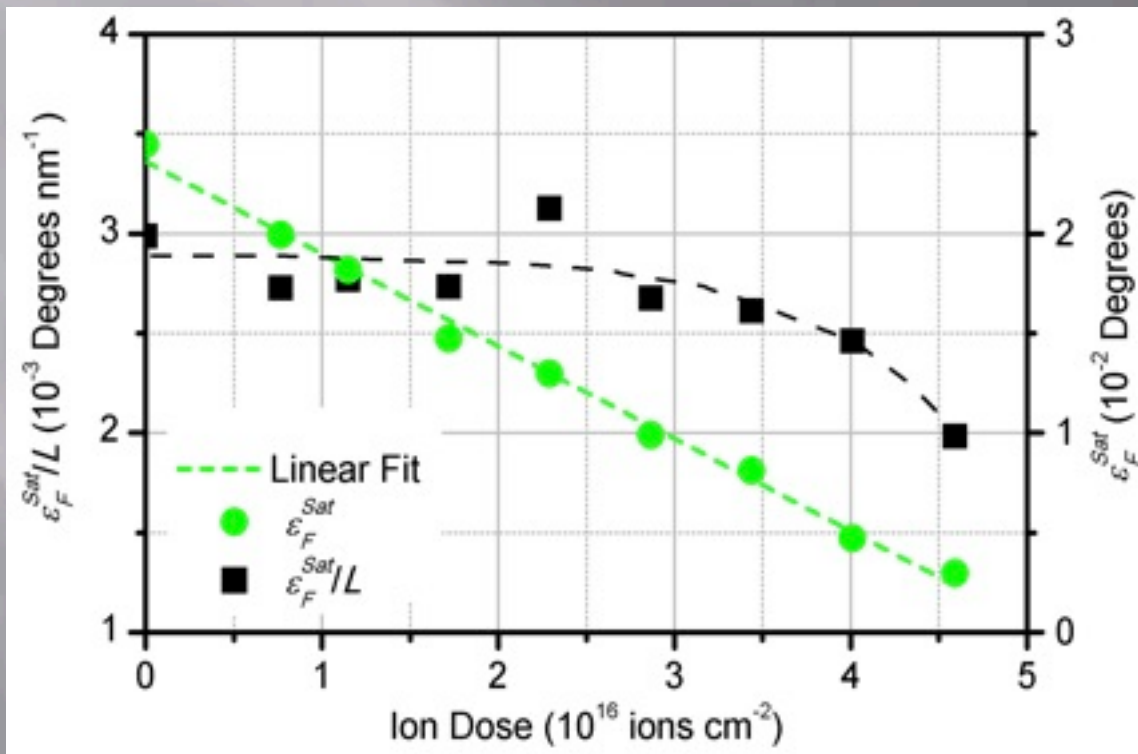
A composite Fe and Fe-Ga pattern. The pattern design is shown in (a), where the dark areas represent the Ga irradiation. XMCD images of the magnetisation reversal sequence are shown in (b)-(f), with an overlay of the pattern design as a guide. The images only show the areas of the film that switch between two successive field steps, which are given along the left side of the images.



Magnetic hysteresis loops measured using Selective Area Stokes Polarimetry (SASP) show the variation in ellipticity angle of the transmitted light with applied field. The inset plots the coercivity of the film vs. ion dose.

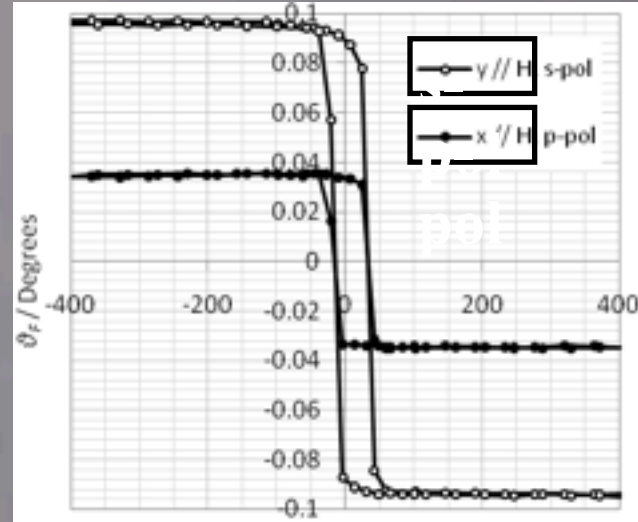


The ellipticity angle of light transmitted through the magnetically saturated Fe and Fe-Ga is inversely proportional to the ion dose due to reducing film thickness. The magnetic circular dichroism is independent of ion dose until the film becomes discontinuous at doses above  $3 \times 10^{16}$  ions  $\text{cm}^{-2}$ . This is illustrated by the black dashed line, which is a guide to the eye only.

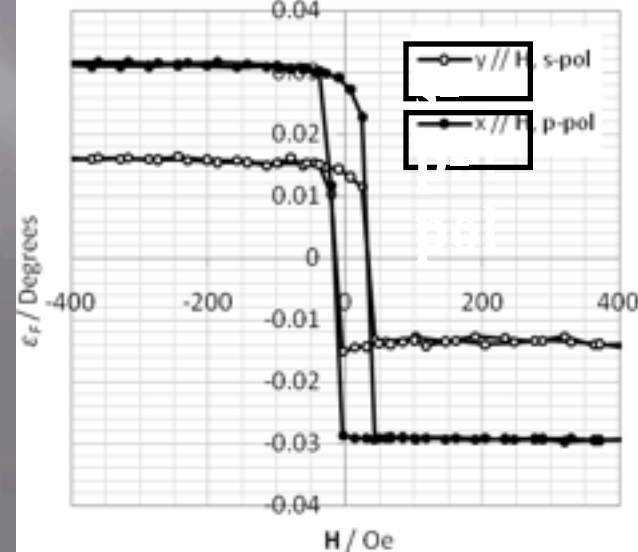


**Magnetic hysteresis behaviour of an Fe thin film obtained using the SASP technique.**  
**Predominantly s- and p-polarised light was incident at an angle of approximately 63° with the magnetic field applied in the plane of incidence. The Faraday rotation induced by the film is shown in (a) and the ellipticity angle in (b).**

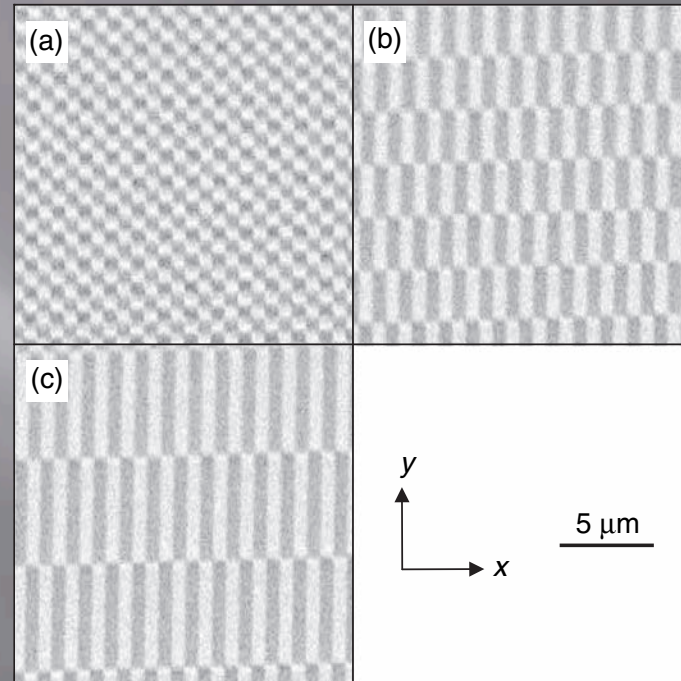
(a)



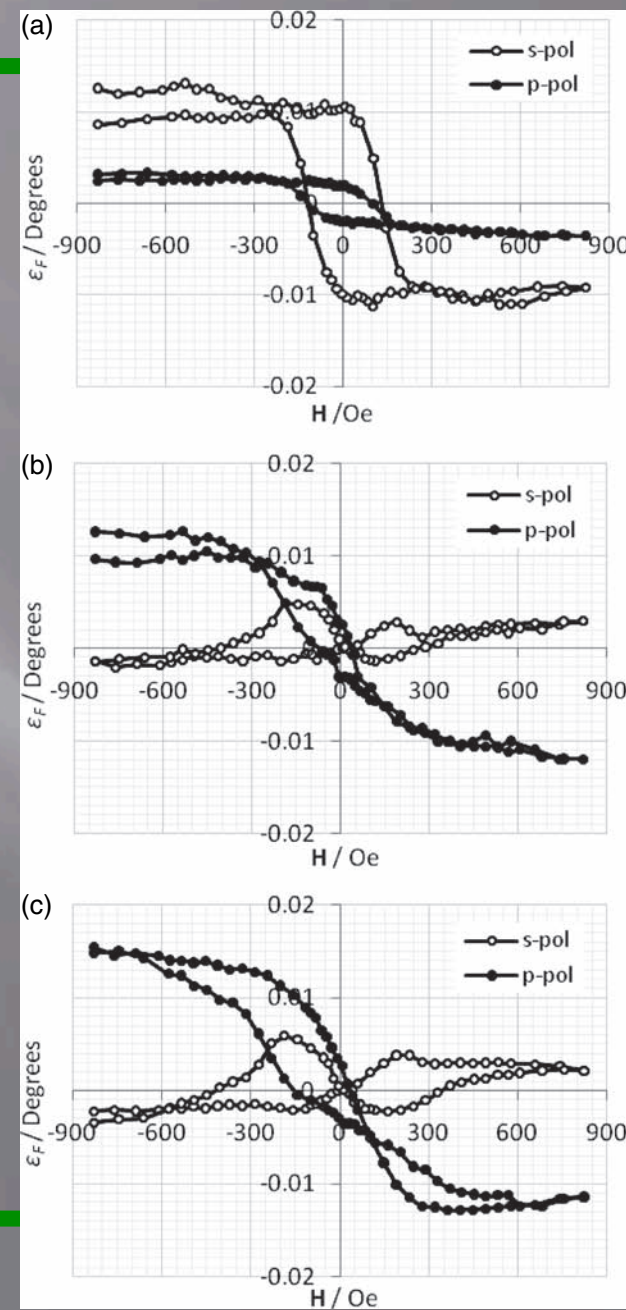
(b)



**SEM images of the chess-board-style patterns etched into an Fe film using an FIB. The dimensions of the Fe (bright) and etched (dark) elements are (a)  $0.725 \mu\text{m} \times 0.725 \mu\text{m}$  (a), (b)  $0.725 \mu\text{m} \times 2.9 \mu\text{m}$  and (c)  $0.725 \mu\text{m} \times 5.8 \mu\text{m}$ .**



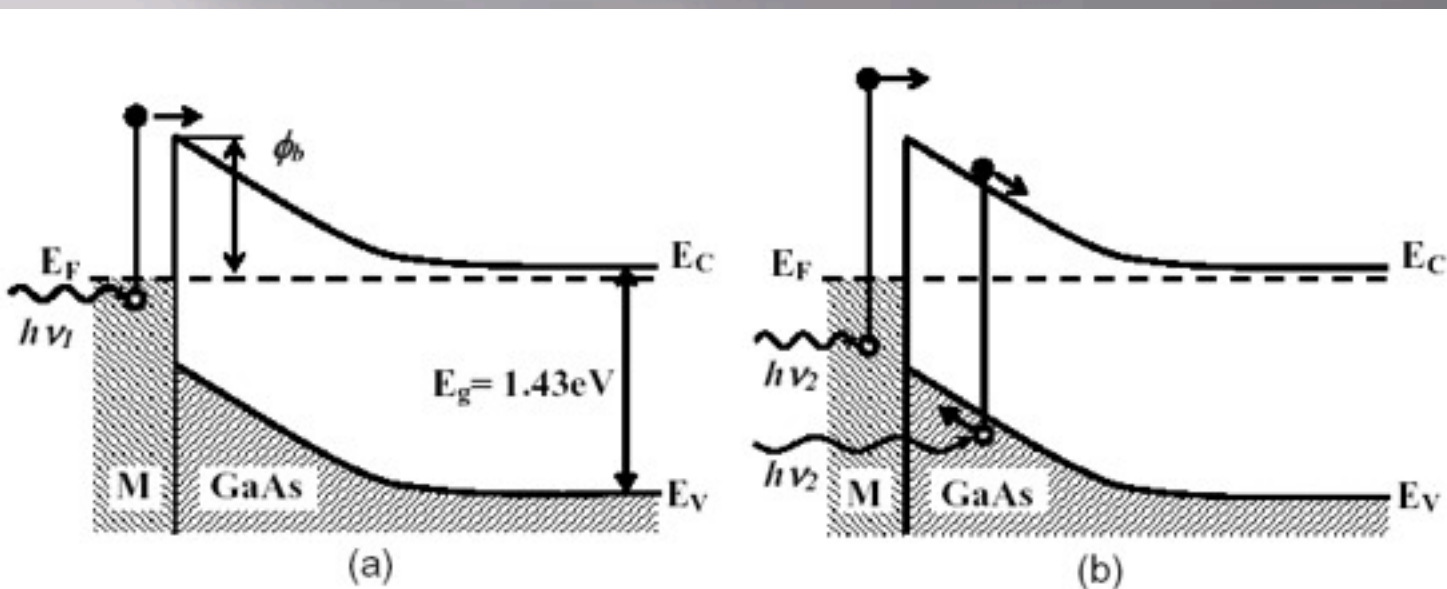
Magnetic hysteresis behaviour of the chess-board-style patterns comprising (a) square, (b) 2.9  $\mu\text{m}$  long and (c) 5.8  $\mu\text{m}$  long elements, with the field applied along the x-axis of the pattern. The loops obtained from the square elements show a relatively ‘normal’ behaviour (apart from the thermal drift in the s-polarised case). As shape anisotropy is introduced, the ellipticity angle no longer represents the magnetisation of the sample.



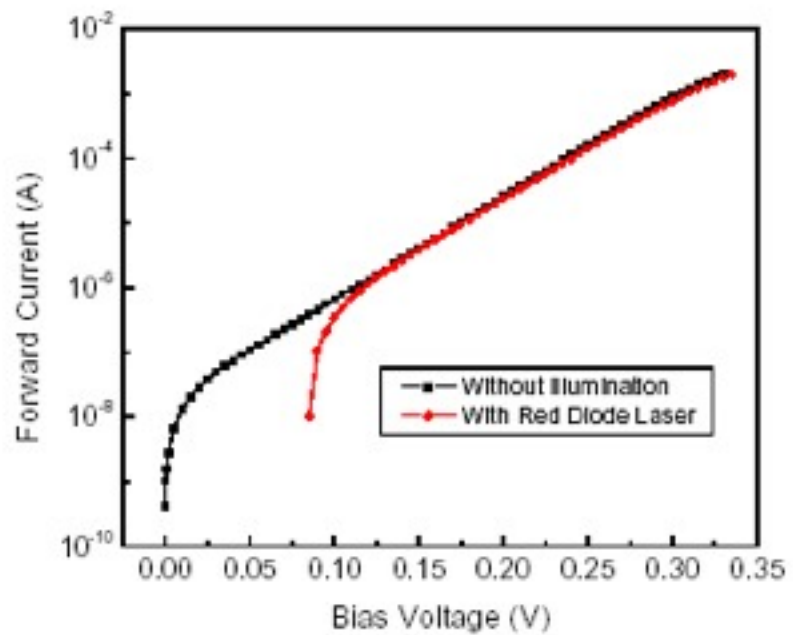
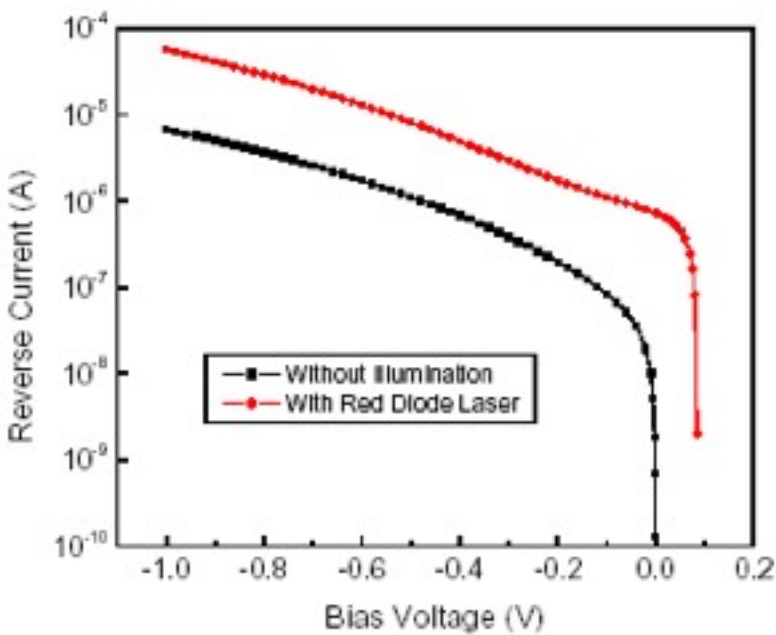
# DETERMINATION OF THE MAGNETIC ASYMMETRY IN PHOTOCURRENTS

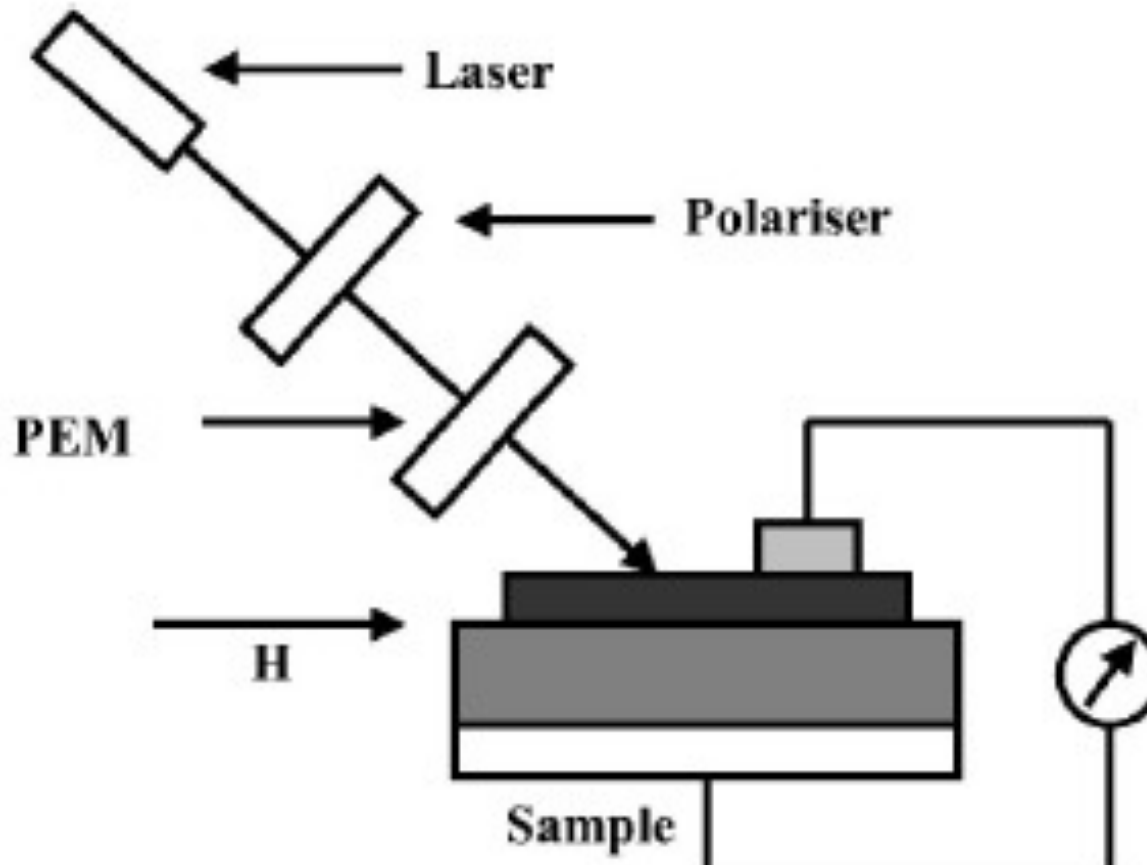
across the Fe/GaAs and Ni/  
GaAs interfaces





# I-C characteristics

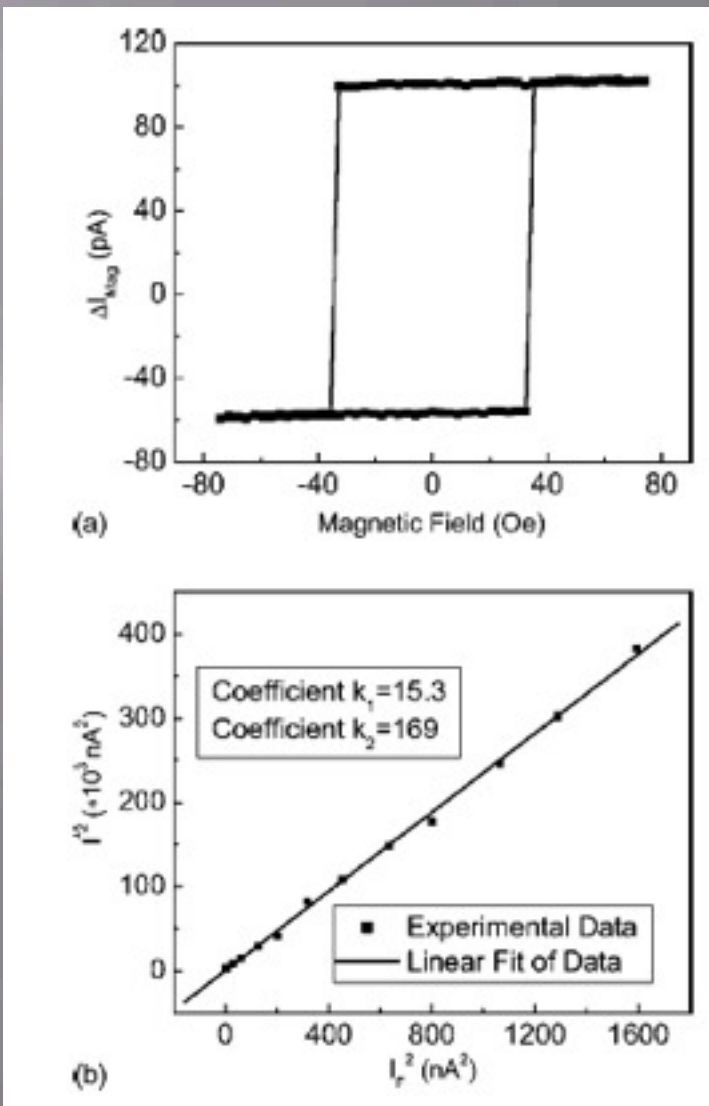


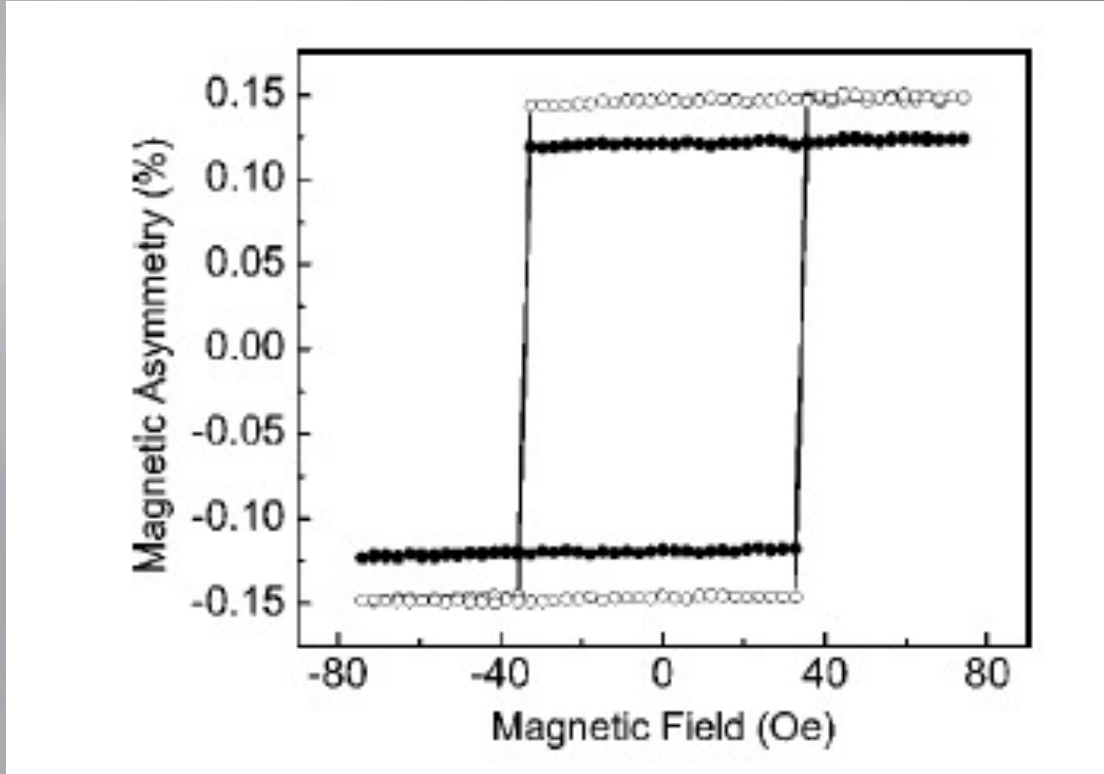


$$I_{\text{Photo}}^2 = k_2^2(I_{2F,Q}^2 + I_{2F,U}^2) + k_1^2 I_F^2.$$

$$A = k_1 \frac{\Delta I_{\text{Mag}}}{I_{\text{Photo}}}.$$

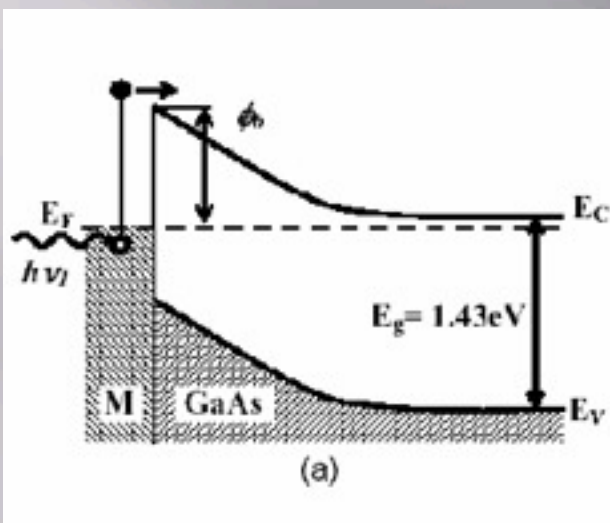
Liu et al. JAP (2005)





The magnetic asymmetry for Fe(12 nm) /GaAs at 45° incidence. The magnetic field was in the plane of incidence and along the magnetic easy axis of the sample. The filled circles are for the measurements using a red diode laser ( $\lambda = 670 \text{ nm}$ ,  $h\nu = 1.85 \text{ eV}$ ), and the open circles using an infrared laser ( $\lambda = 1064 \text{ nm}$ ,  $h\nu = 1.17 \text{ eV}$ ).





[7.20] M. M. Steiner, R. C. Alberts and L. J. Sham, Phys. Rev. B 45, 13272 (1992).

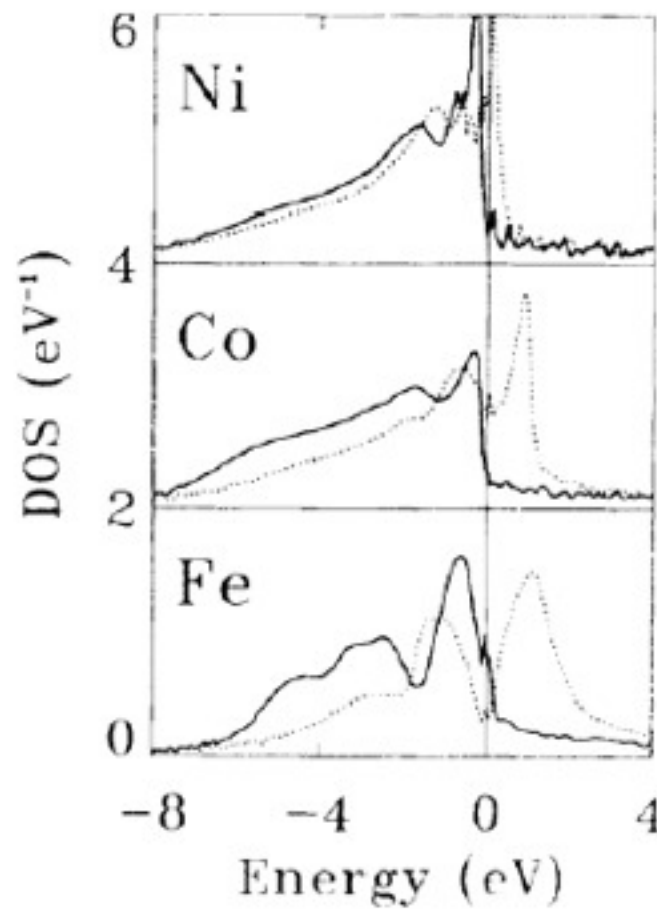
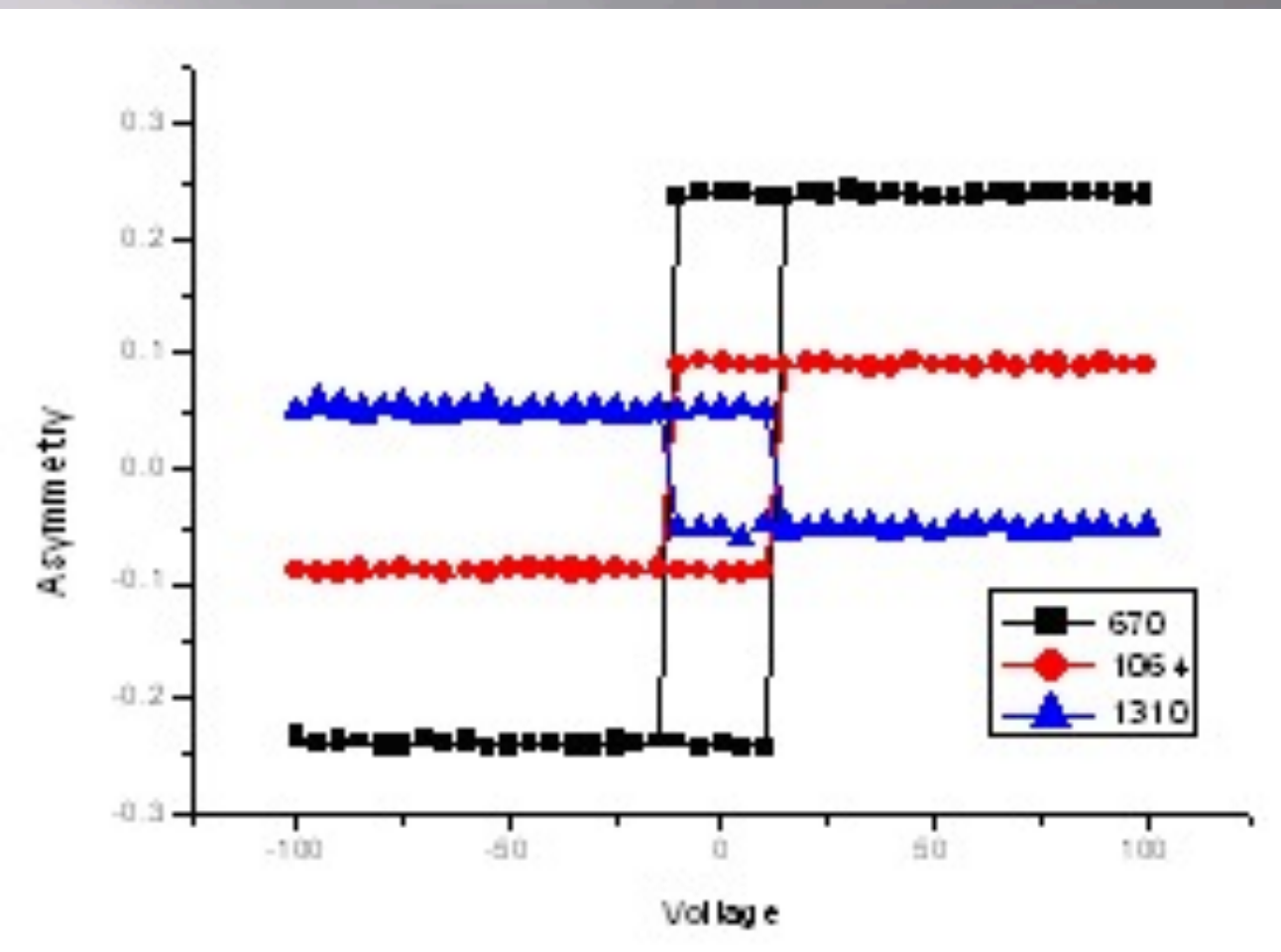


**Figure 7.1.2.2:** The spin-resolved density of states (DOS) for the 3d ferromagnets (solid/dotted line = majority/minority states). The energy has been shifted so the Fermi energy is at zero energy.<sup>7.20</sup>



# POLARISATION CHANGES IN CELLULAR DYNAMICS OF CARDIOVASCULAR CELLS

a proof of concept





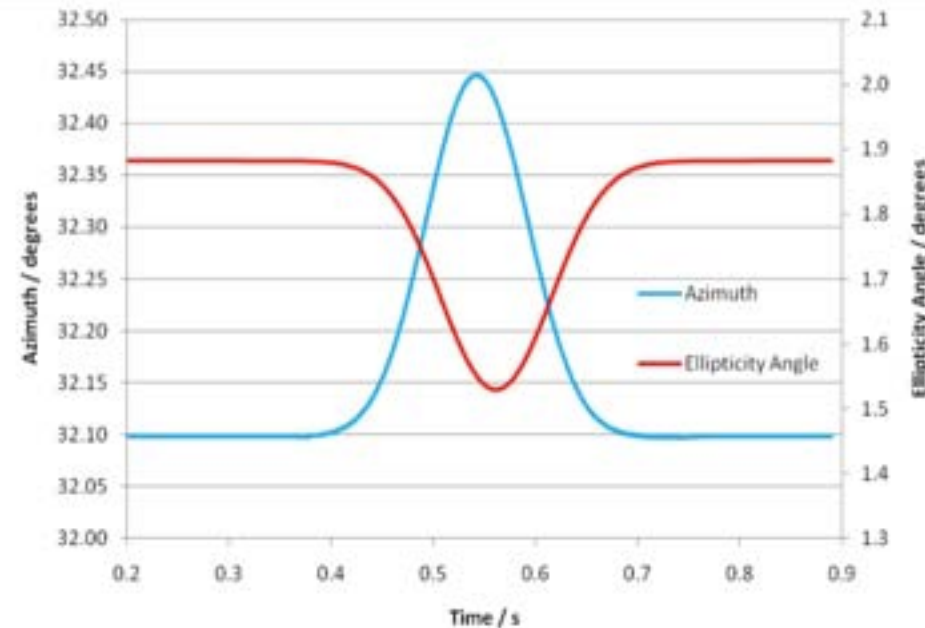
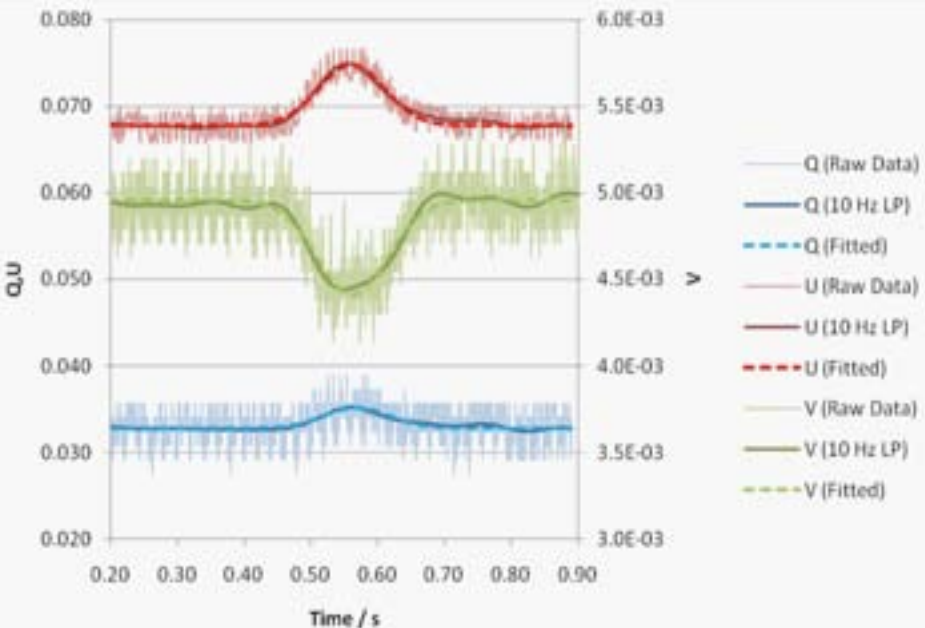
P. Cook, T.H. Shen (Salford)

H. Zhang and M. Lei (Manchester)





polarisation changes during a contraction  
of a mouse cardiovascular cell.



# Summary/Future work

- A methodology is developed to measure the full state of polarisation of light with very high sensitivity.
- MO effects of magnetic nanowire arrays have been characterised.
- Current/Future work- a systematic study of structures from mesoscopic to ‘nanoscopic’ based on patterned thin films; modelling; non-linear optical characteristics.
- The development of a Stokes polarimetric microscope with high sensitivity and frame speed for the observation of dynamic cellular processes.

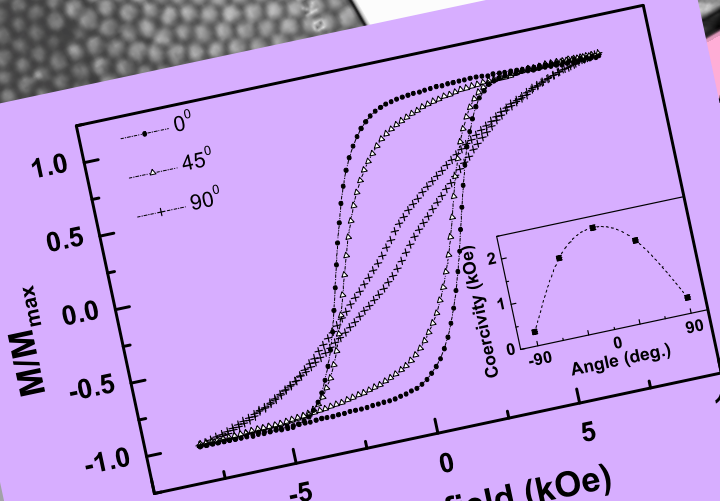


# Acknowledgement

- Dr. M. Spangenberg, Dr. T.Zhang, Dr. J. R. Neal, Prof. Y. Peng, Prof. W.Li, Dr. Y. Liu, Dr. W.Guan, Prof. J. Zhang, Dr. J. Thompson, Dr. P. Cook, Dr. L. Qin, Dr. N. Wang
- Miss A. Heyes
- Dr. N. Takahashi, Dr. A.E.R. Malins, Dr. X. Zhao
- Dr. G. A. Jones, Prof. P. J. Grundy, Dr. C. A. Faunce, Mr. B. Ashworth
- Dr. Morton (ALS), Dr. E. Arenholz (ALS), Dr. A.D.L. Kilcoyne (ALS), Prof. C. Binns (Leicester)



# Thank you!



We acknowledge the financial support of HEFCE and the University of Bristol.

